Chapter 5

Encapsulation and α-Helical Folding of 9-Residue Peptide within a Hydrophobic Dimeric Capsule of a Bowl-shaped Host

Abstract

A dimeric capsule of coordination bowl could encapsulate nine-residue peptide (Trp-Ala-Glu-Ala-Ala-Ala-Glu-Ala-Trp) within the large hydrophobic cavity in water, and stabilized α-helical conformation of bound peptide. NMR titration experiment revealed that monomeric bowl sequentially recognized two Trp residues at the both terminals of the peptide through bowl:peptide = 1:1 to 2:1 complex. However, the 1:1 and the 2:1 species existed in equilibrium even in the presence of excess bowl. It was found that formation of the 2:1 complex, two bowls covered the whole of the peptide, was facilitated in the presence of $NaNO_3$ due to increase of hydrophobic interaction between Trp residues and cavity of bowl. Furthermore, we discussed α-helical conformation within the dimeric capsule from detailed NOESY analysis.

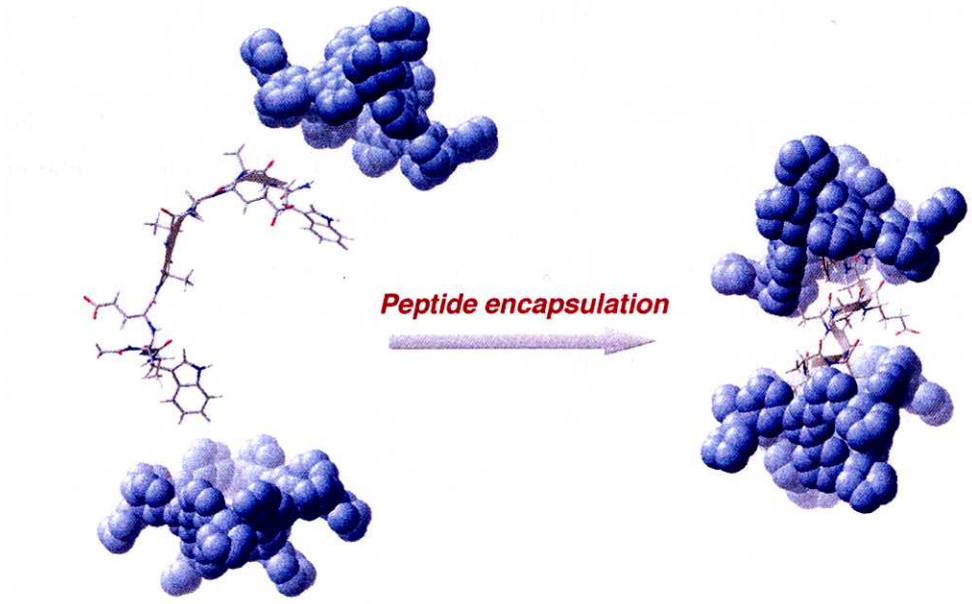

5.1 Introduction

Peptide engineering has been realizing the artificial construction of molecules and materials with sophisticated functions by utilizing the latent nature of peptides to be spontaneously folded into their secondary structures.[1] This research field is rapidly developing through the understanding of the mechanism and design principle of peptide folding, which is still a major interest in peptide chemistry. Extensive studies have been made on the formation of peptide secondary structures from de novo designed oligopeptides.[2,3] Unlike those incorporated in a protein scaffold, however, short peptide fragments cannot form stable secondary structures.[4] Hence the folding of secondary structures of peptides has been often achieved by cross-linking of side-chains via covalent bonding and metal-coordination.[5,6]

Another approach for the stabilization of secondary structures is peptide encapsulation within a hydrophobic cavity. This strategy is reminiscent of nature's system since the secondary structures are sustained only by weak interactions in the cavity. However, oligopeptide encapsulation by synthetic hosts is a difficult task because most of host molecules, such as cyclodextrins and calixarenes, have relatively small cavity that can bind only one small organic molecule. In previous examples of peptide recognition, two binding sites had to be covalently linked.[7] For example, Breslow and co-workers prepared cyclodextrin dimers and demonstrated the stabilization of α-helix coformation of a peptide containing unnatural amino acids as recognition sites.[7b]

The most efficient way to provide cavities large enough to bind peptides is the construction of large hosts by molecular self-assembly. Cages, bowls, and capsules with extraordinarily large cavities have been prepared by self-assembly through hydrogen or coordination bonds.[8] Atwood and Rebek reported the assembly of a nanocapsule from six molecule of resorcin[4]arenes via 60 hydrogen bonds, though the recognition of large molecules by the nanocapsule has been not achieved.[9] Recently, Rebek and co-workers demonstrated the helical folding of linear alkanes by encapsulation within a cylindrical capsule that assembled from two cavitands.[10] We[11] and others[12] have been showing the remarkable potential of metal-directed self-assembly for the construction of discrete host compounds with large cavities. Among them, Pd^{II}- or Pt^{II}-linked roughly spherical M_6L_4 type cage binds variety of large neutral organic guests in a surprisingly efficiently fashion.[13]

Metal-linked M_6L_4 bowl (**1**) also shows unique host properties.[14] It dimerizes into a hydrophobic capsule to bind up to four large guests in the capsule. For example, encapsulation of four molecules of *m*-terphenyl or *cis*-stilbene have been confirmed by X-ray crystallographic analysis and NMR.[14b] In expectation of binding peptides within the dimeric

capsule, we recently examined the recognition of nine-residue peptide with the bowl **1** as described in chapter 4. Although the dimeric capsule was not formed, the bowl **1** induced α-helical conformation of the peptide in an aqueous solution in the presence of $CHCl_3$ (1v/v%) to give a 1:1 complex. In this complex, hydrophobic face in the α-helix was deeply accommodated in the cavity of **1**. $CHCl_3$ seems to be co-enclathrated with the peptide. In the absence of $CHCl_3$, the conformation of the peptide was ambiguous and hardly analyzed.

To encapsulate the peptide within the dimeric capsule of **1**, we have examined a salt effect because the host-guest hydrophobic interaction is expected to increase with increasing ion strength of the solution. Accordingly, we describe here the encapsulation of nine-residue peptide **2** within the large hydrophobic cavity of Pt^{II}-bowl **1** dimer in $NaNO_3$ aqueous solution. Detailed NMR study shows that (1) the dimerization of bowl **1** is induced by complexation with two Trp residues at the both ends of **2**, (2) the formation of the dimeric structure occurs stepwise via 1:1 complex, and (3) the peptide accommodated in the dimeric capsule adopts α-helical conformation.

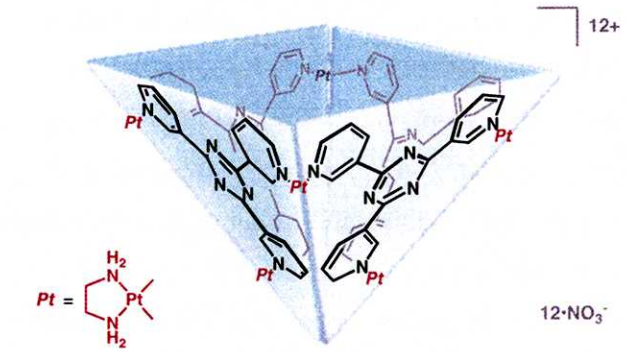

1

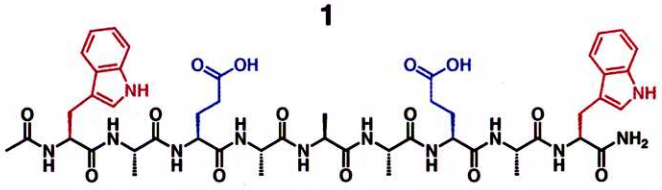

2

5.2 Results and Discussion

5.2.1 Site-selective recognition of 9-residue peptide

The association of the 9-residue peptide (**2**) with Pt^{II}-bowl **1** ,discussed in previous chapter, was studied by NMR titration without chloroform. The sequential assignment of **2** in **1** was carried out by TOCSY and NOESY measurements. Upon the addition of **1** into the aqueous solution of **2**, the colorless solution turned yellow indicating the charge-transfer interaction

between the electron-rich Trp residues and the electron deficient bowl. It was found that the binding of the two Trp residues (Trp1 and Trp9) with the bowl was not simultaneous but sequential. Firstly, Trp9 at the C-terminal was bound to give a 1:1 complex and, secondly, the complexation of Trp1 at N-terminal follows to give a 2:1 complex.

The ^{1}H NMR titration showed that, at **1**:**2** = 1:1, Hβ signal of Ala8 was significantly up-field shifted compared with other Ala residues (Figure 1). Upon further addition of **1**, the up-field shift of this signal was saturated at **1**:**2** = ca 2:1, while those of other Ala Hβ signals were not saturated. The signal of Ala2 near the N-terminal was much less shifted up-field. This suggests that C-terminal of **2** was preferentially recognized to give a 1:1 complex as an intermediate. Association constant for the 1:1 complexation was estimated to be roughly 10^4–10^5 M^{-1} from NMR titration. This site-selectivity was supported by two control experiments. The association of **1** with Trp9-Ala9 mutated peptide, Ac-Trp-Ala-Glu-Ala-Ala-Ala-Glu-Ala-*Ala*-NH_2 (**3**), and Trp1-Ala1 mutated peptide, Ac-*Ala*-Ala-Glu-Ala-Ala-Ala-Glu-Ala-Trp-NH_2 (**4**) was examined. UV-vis titrations showed that peptide **4** was recognized five times stronger than **3** (Table 1), consistent with the C-terminal selective recognition of **2**. We also prepared Glu7–Lys7 mutated peptide. The complexation at the C-terminal should be disturbed since the positive charge of Lys7 repulses the cationic bowl **1**. As a result, affinities at both terminals were comparable, as indicated by simultaneous up-field shifting of Ala2 and Ala8 (Figure 2).

5.2.2 Encapsulation of **2** within a dimeric capsule of **1**

As mentioned above, 2:1 complexation was observed in the presence of excess **1**. The Hβ signals of not only Ala8 but also Ala2 were up-field shifted in the presence of 5 equiv of **1** (Figure 1d), suggesting that both terminals were bound within the cavity of **1**. To confirm the formation of 2:1 species, we estimated the molecular size of complexes from DOSY measurements. From DOSY, the diffusion coefficient of control peptide **4** in the presence of 4 equiv of bowl **1** was 1.26 x 10^{-10} m^2s^{-1}. This value should reflect the 1:1 complex because peptide **4** has only one Trp residue and can form only 1:1 complex with **1**. The diffusion coefficient of peptide **2** in the presence of 4 equiv of bowl **1** (1.06 x 10^{-10} m^2s^{-1}) was smaller than that of **4** (Figure 3). This result indicated the formation of a complex larger than the 1:1 complex. Namely, 2:1 species is suggested.

The Job's plot by UV-vis measurements indicated that the 1:1 and the 2:1 species existed in equilibrium even in the presence of excess **1**.[15] The plot exhibited a peak at approximately 0.6 (Supporting Information), being smaller than 0.66 for ideal 2:1 complexation (Figure 4). Assuming that the maximum up-field shift of Ala2 is comparable to that of Ala8, we

estimated the ratio of the 1:1 and 2:1 complexes to be about 40:60 from $\Delta\delta_{Ala2}/\Delta\delta_{Ala8}$ ratio at [**1**] = 10 mM and [**2**] = 2 mM (Figure 1d).

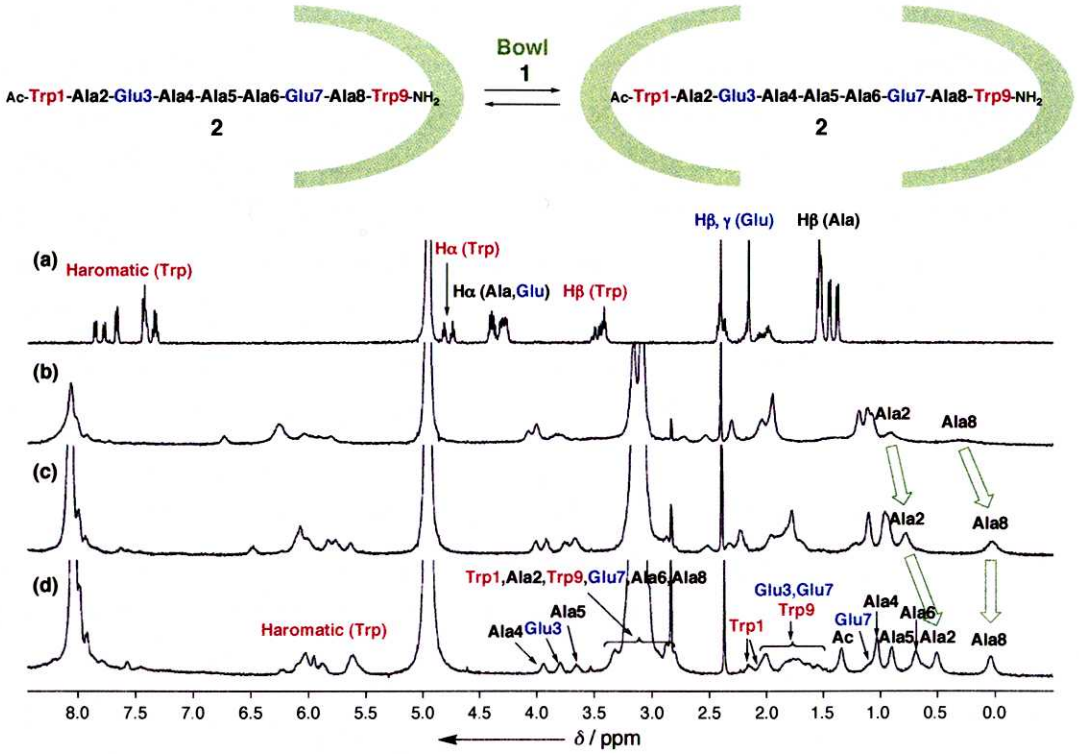

Figure 1. ^{1}H NMR spectra (500 MHz, D_2O, 27 °C) of **2** ([**2**] = 2 mM) in 100 mM phosphate buffer (pH 6.8) and **1** (a) [**1**] = 0 mM, (b) 2 mM, (c) 4 mM, (d) 10 mM.

Table 1. Association constants of **1** with control peptides in water

Peptides	K_a (M^{-1})[a]
Ac-**Trp**-Ala-Glu-Ala-Ala-Ala-Glu-Ala-Ala-NH_2 (**3**)	1.6 (± 0.2) x 10^4
Ac-Ala-Ala-Glu-Ala-Ala-Ala-Glu-Ala-**Trp**-NH_2 (**4**)	8.6 (± 1.2) x 10^4

[a] Measured by UV-vis titration at 20 °C in 10 mM phosphate buffer (pH 6.8).

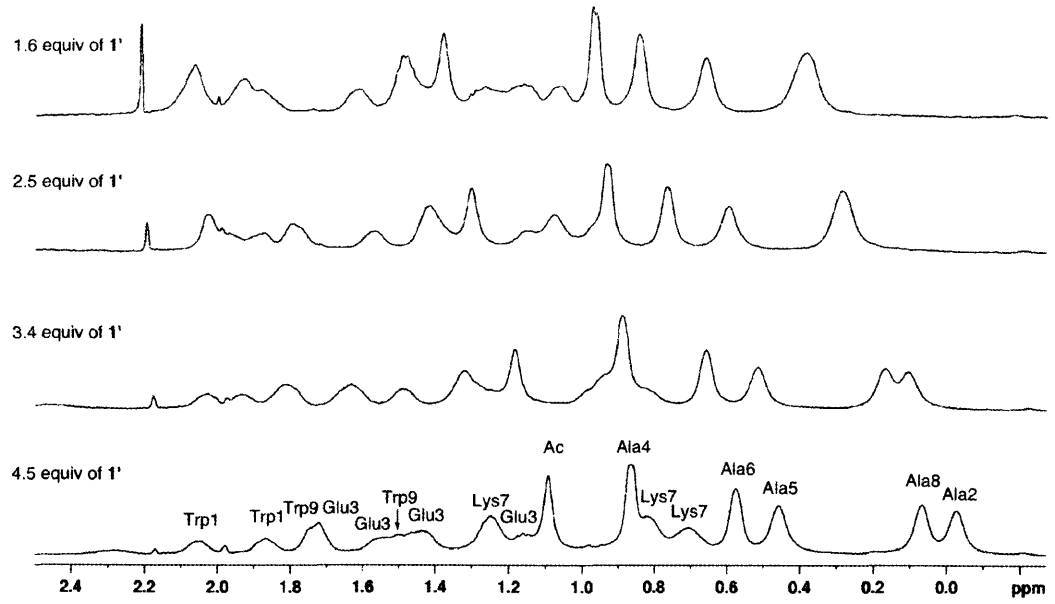

Figure 2. ^{1}H NMR titration of Ac-Trp-Ala-Glu-Ala-Ala-Ala-Lys-Ala-Trp-NH_2 with Pd(II)-bowl **1'**. Sequential assignment of final condition (4.5 equiv of **1'**) was carried out by the same method in the case of peptide **2** and Pt(II)-bowl **1**.

The Job's plot by UV-vis measurements indicated that the 1:1 and the 2:1 species existed in equilibrium even in the presence of excess **1**.[15] The plot exhibited a peak at approximately 0.6 (Supporting Information), being smaller than 0.66 for ideal 2:1 complexation (Figure 4). Assuming that the maximum up-field shift of Ala2 is comparable to that of Ala8, we estimated the ratio of the 1:1 and 2:1 complexes to be about 40:60 from $\Delta\delta_{Ala2}/\Delta\delta_{Ala8}$ ratio at [**1**] = 10 mM and [**2**] = 2 mM (Figure 1d).

5.2.3 Stabilization of the 2:1 complex by addition of $NaNO_3$

To stabilize the 2:1 complex formation, we studied a salt effect since the host-guest hydrophobic interaction is expected to increase with increasing ion strength.[16] The addition of $NaNO_3$ induced further up-field shift of Ala2 signal of **2** (Figure 5), suggesting that formation of the 2:1 complex became dominant. Under the conditions of Figure 3c ([**1**] = 10 mM [**2**] = 2.5 mM. [$NaNO_3$] = 400 mM), the ratio of the 1:1 and the 2:1 complexes was estimated to be about 20:80.

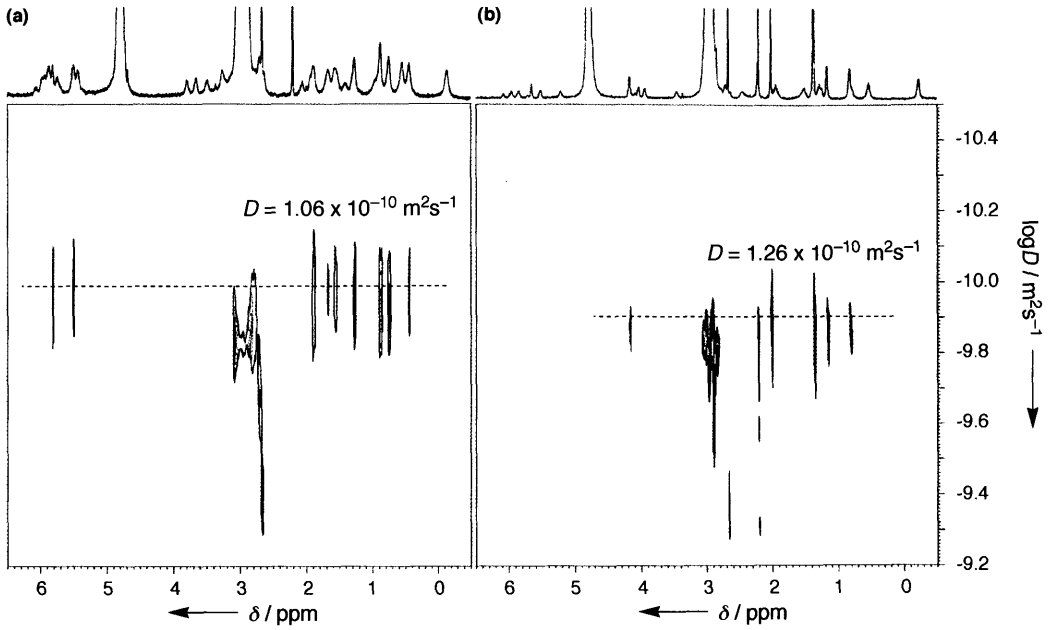

Figure 3. DOSY spectra (500 MHz, D_2O, 27 °C) of 4 equiv of **1** in 100 mM phosphate buffer (pH 6.8) and (a) peptide **2** ([**2**] = 1.9 mM), (b) peptide **4** ([**4**] = 1.8 mM).

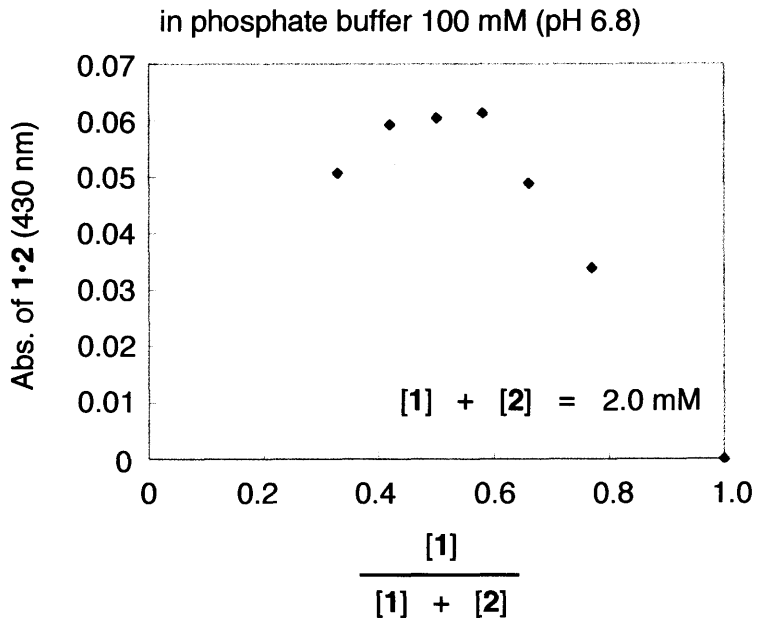

Figure 4. Job's plot. Concentration of complex was estimated from CT absorption around 350-500 nm that is specific to the complex.

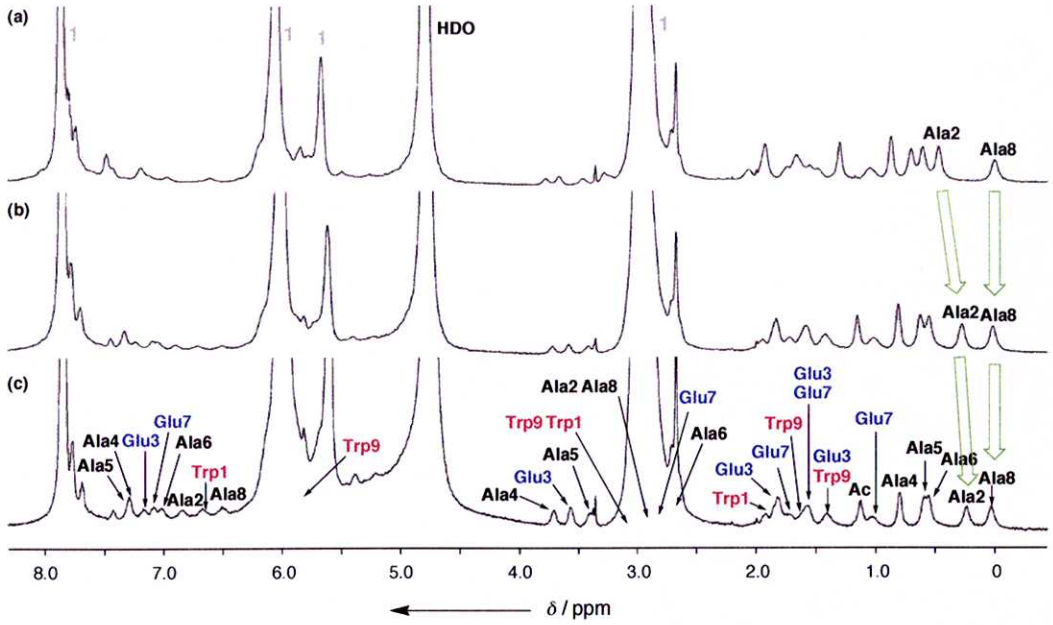

Figure 5. ^{1}H NMR spectra (500 MHz, H_2O/D_2O = 9/1, 27 °C) of **1** ([**1**] = 10 mM) and **2** ([**2**] = 2.5 mM) in 100 mM phosphate buffer (pH 6.8) in the presence of $NaNO_3$ (a) 0 mM, (b) 200 mM, (c) 400 mM.

5.2.4 Stabilization of α-helical structure of **2** within the dimeric capsule of **1**

In the absence of $NaNO_3$, the conformation of peptide **2** was hardly analyzed because of rapid equilibration on the NMR timescale between two different conformers in the 1:1 and 2:1 complexes and also for relatively loose host-guest interaction. Upon the addition of $NaNO_3$ (400 mM), the 2:1 complex was dominant and the conformation of the peptide was fixed. Thus, the secondary structure of peptide **2** in the 2:1 complex was analyzed by NOESY experiments. Circular dichroism (CD) spectrometry, generally used for the characterization of peptide secondary structures, was not useful because of fatal interference of CD of **2** by strong absorption of **1** around 200-250 nm.

In the NOESY spectrum, we observed sequential NOEs $d_{NN}(i,i+1)$ and several medium range NOEs: for example, $d_{\alpha\beta}(i,i+3)$, $d_{\alpha N}(i,i+3)$, and $d_{\alpha N}(i,i+4)$. The observation of these NOEs is characteristic to typical α-helix conformation (Figure 6).[17] Only a few unreasonable NOEs for the α-helical conformation were observed because of the co-existence of some minor conformers. Since CD measurement showed the unordered structure of free peptide **2** in water, the α-helical conformation of **2** was obviously induced by the encapsulation of **2** within the dimeric capsule of **1**.

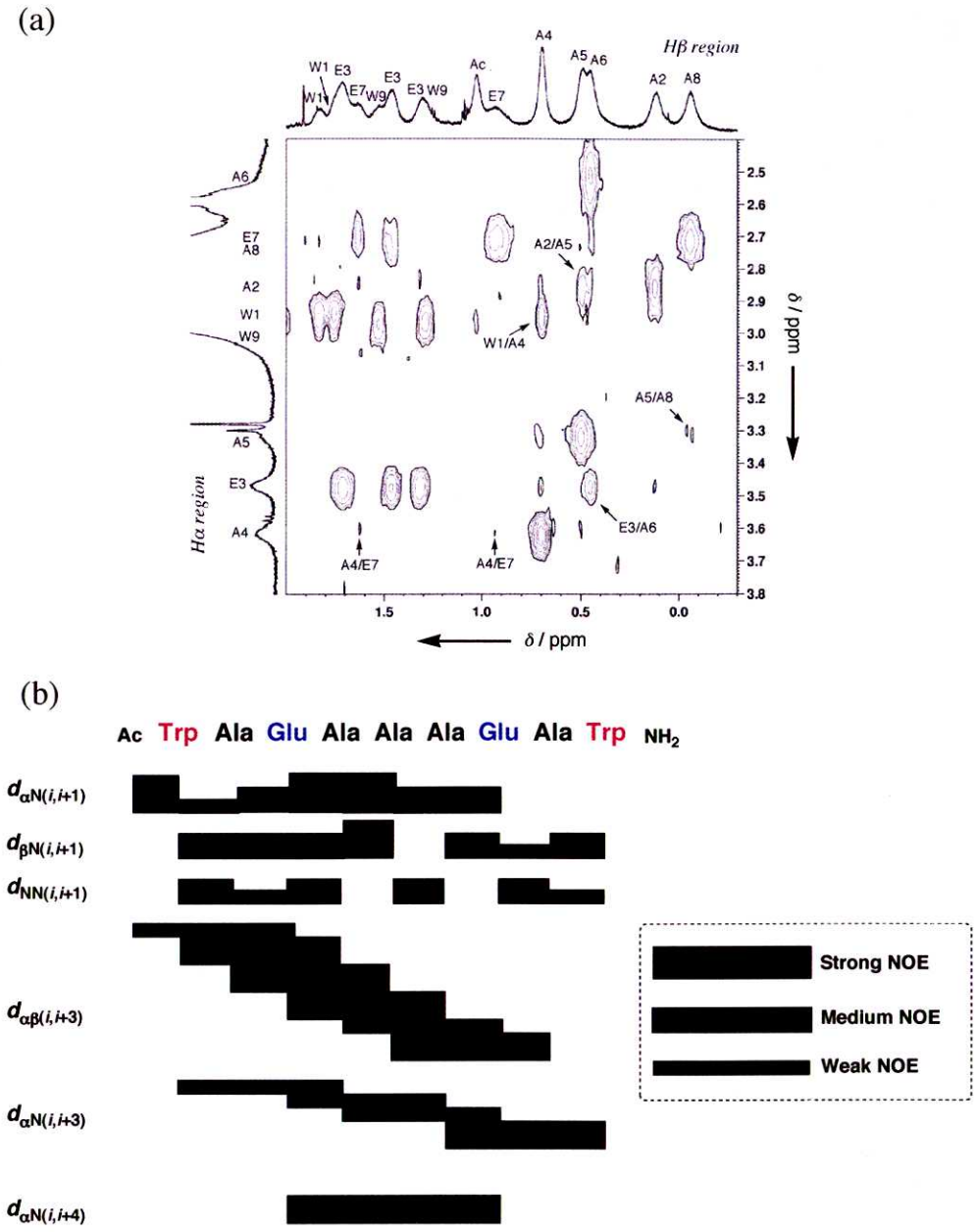

Figure 6. (a) Selected NOESY spectrum (600 MHz, H_2O/D_2O = 9/1, 27 °C) of **1** ([**1**] = 10 mM) and **2** ([**2**] = 2.5 mM) in 100 mM phosphate buffer (pH 6.8) at the presence of 400 mM $NaNO_3$. (b) NOE correlations for the bound peptide **2** in the same condition.

5.2.5 Proposed structure of helical peptide **2** and the dimeric capsule of **1**

To estimate the geometry of **2** in the 2:1 complex, chemical shifts of the residues were compared with those of free **2**. All signals of **2** exhibited negative Δδ values from -0.6 to -2.3 ppm (Figure 7). This observation indicates that the whole of **2** is covered by the dimeric capsule of **1**. Hβ protons near terminal Trp residues were much more up-field shifted than others, indicating the tight and deep accommodation of the residues near both terminals within bowl **1**. For example, Δδ of the Hβ of Ala2 (-1.20 ppm) and Ala8 (-1.38 ppm) was larger than that of Ala4 (-0.62 ppm), Ala5 (-0.83 ppm) and Ala6 (-0.87 ppm). The up-filed shift of the middle residues also indicates the folding of the peptide into a compact form. Based on these observations, we proposed the encapsulation of peptide **2** in α-helical conformation within the hydrophobic cavity of the dimeric capsule as shown in Figure 8.

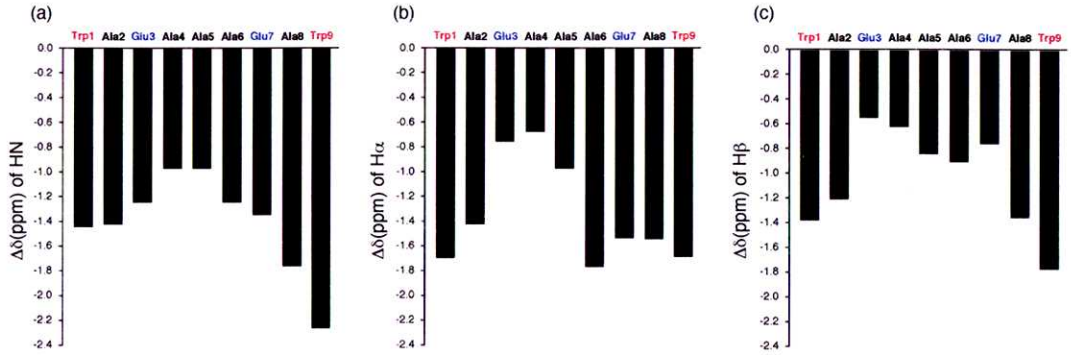

Figure 7. Up-field chemical shifts for **2** ([**2**] = 2.5 mM) with **1** ([**1**] = 10 mM) in 100 mM phosphate buffer (pH 6.8) at the presence of 400 mM $NaNO_3$. These value of each residues was compared with chemical shifts of extended chain.

5.2.6 Dynamic host-guest assembly controlled by media

Dynamic feature of the bowl-peptide complexation deserves attention. In the aqueous solution of **2** (2.5 mM) and **1** (7.5–10 mM), the peptide conformation and the complexation ratio are ambiguous. Addition of $NaNO_3$ induced the dominant formation of the 2:1 complex in which peptide **2** in α-helical conformation is encapsulated in the dimeric capsule of **1**, as described above. On the other hand, we have previously reported the dominant formation of a 1:1 complex in the presense of $CHCl_3$, where peptide **2** in α-helical conformation is co-enclathrated with $CHCl_3$ in the monomeric bowl. There have appeared many examples of dynamic molecular assembly in which guests induce host frameworks.[18] In contrast, the present host-guest system varies the assembly manner depending on media conditions ($CHCl_3/H_2O$ vs $NaNO_3/H_2O$). Such a dynamic host assembly responsive to media provides a prototype for a new type of external stimuli-responsive molecular assembly.

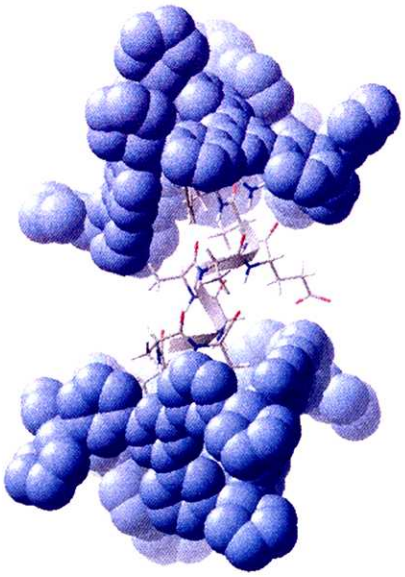

Figure 8. The proposed structure of **2** and dimeric capsule of **1**. Dimeric capsule of **1** and peptide **2** are represented by space-filling and cylindrical models, respectively.

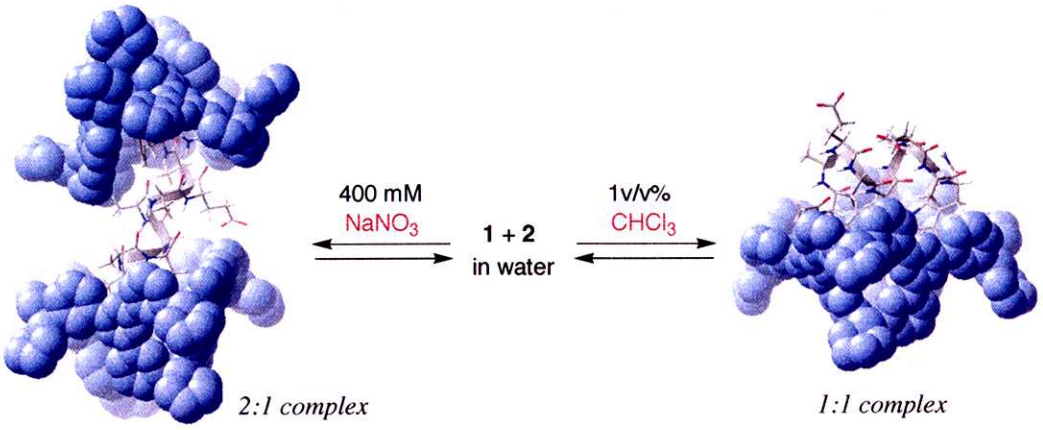

5.3 Conclusion

In conclusion, we demonstrated that 9-residue peptide **2** was encapsulated within the large hydrophobic cavity of dimeric capsule assembled from two coordination Pt^{II} bowl complex **1**. The driving forces of the formation of the dimeric capsule are hydrophobic and charge-

transfer interaction between **1** and Trp residues at both terminals of **2**. Furthermore, we observed the stabilization of the α-helical conformation of **2** within the large hydrophobic cavity of the dimeric capsule from NOESY experiments. Most interestingly, the approach in this work for the stabilization of secondary structure mimics biological systems. Thus, other secondary structures, such as β-strand, β-hairpin, and turn structures, can be stabilized within hydrophobic pocket of various coordination structures synthesized by our group.[11] Moreover, when we design larger cavity enough to accommodate a whole or part of protein molecules, this strategy is expected to be applicable to not only the stabilization of ephemeral tertiary structure but also studies for the pathway of protein folding.

5.4 Experimental Section

Materials, peptide synthesis, procedure of UV titration, NMR measurements, Job's plot and structural calculation by CNS were described in General Experimental Section. Synthesis of the bowl-shaped host was described in Chapter 4.

5.5 References

1 (a) W. A. Petka, J. L. Harden, K. P. McGrath, D. Wirtz, D. A. Tirrell, *Science* **1998**, *281*, 389–392. (b) D. T. Bong, T. D. Clark, J. R. Granja, M. R. Ghadiri, *Angew. Chem.* **2001**, *113*, 1016–1041. *Angew. Chem. Int. Ed.* **2001**, *40*, 988–1011. (c) J. D. Hartgerink, E. Beniash, S. I. Stupp, *Science* **2001**, *294*, 1684–1688. (d) N. Sakai, S. Matile, *Chem. Commun.* **2003**, 2514–2523.

2 De novo design of helix: (a) K. R. Shoemaker, P. S. Kim, E. J. York, J. M. Stewart, R. L. Baldwin, *Nature*, **1987**, *326*, 563–567. (b) S. Marqusee, R. L. Baldwin, *Proc. Natl. Acad. Sci. USA* **1987**, *84*, 8898–8902. (c) P. C. Lyu, M. I. Liff, L. A. Marky, N. R. Kallenbach, *Science* **1990**, *250*, 669–673. (d) S. Padmanabhan, S. Marqusee, T. Ridgeway, T. M. Laue, R. L. Baldwin, *Nature* **1990**, *344*, 268–270. (e) D. H. Appella, L. A. Christianson, D. A. Klein, D. R. Powell, X. Huang, J. J. Barchi Jr, S. H. Gellman, *Nature*, **1997**, *387*, 381–384. (f) T. M. Iqbalsyah, A. J. Doig, *J. Am. Chem. Soc.* **2005**, *127*, 5002–5003.

3 De novo design of β-sheet structures: (a) M. R. Ghadiri, J. R. Granja, R. A. Milligan, D. E. McRee, N. Khazanovich, *Nature*, **1993**, *366*, 324–327. (b) F. J. Blanco, M. A. Jiménez, J. Herranz, M. Rico, J. Santoro, J. L. Nieto, *J. Am. Chem. Soc.* **1993**, *115*, 5887–5888. (c) T.

S. Haque, S. H. Gellman, *J. Am. Chem. Soc.* **1997**, *119*, 2303–2304. (d) J. Venkatraman, G. A. N. Gowda, P. Balaram, *J. Am. Chem. Soc.* **2002**, *124*, 4987–4994. (e) S. M. Butterfield, W. J. Cooper, M. L. Waters, *J. Am. Chem. Soc.* **2005**, *127*, 24–25.

4 B. H. Zimm, J. K. Bragg, *J. Chem. Phys.* **1959**, *31*, 526–535.

5 Covalent bonding: (a) D. Y. Jackson, D. S. King, J. Chmielewski, S. Singh, P. G. Schultz, *J. Am. Chem. Soc.* **1991**, *113*, 9391–9392. (b) C. Bracken, J. Gulyás, J. W. Taylor, J. Baum, *J. Am. Chem. Soc.* **1994**, *116*, 6431–6432. (c) E. Cabezas, A. C. Satterthwait, *J. Am. Chem. Soc.* **1999**, *121*, 3862–3875. (d) C. E. Schafmeister, J. Po, G. L. Verdine, *J. Am. Chem. Soc.* **2000**, *122*, 5891–5892. (e) R. N. Chapman, G. Dimartino, P. S. Arora, *J. Am. Chem. Soc.* **2004**, *126*, 12252–12253.

6 Metal-coordination: (a) M. R. Ghadiri, C. Choi, *J. Am. Chem. Soc.* **1990**, *112*, 1630–1632. (b) F. Ruan, Y. Chen, P. B. Hopkins, *J. Am. Chem. Soc.* **1990**, *112*, 9403–9404. (c) M. J. Kelso, H. N. Hoang, W. Oliver, N. Sakolenko, D. R. March, T. G. Appleton, D. P. Fairlie, *Angew. Chem.* **2003**, *115*, 437–440. *Angew. Chem. Int. Ed.* **2003**, *42*, 421–424. (d) A. Ojida, M. Inoue, Y. Mito-oka, I. Hamachi, *J. Am. Chem. Soc.* **2003**, *125*, 10184–10185.

7 (a) R. Breslow, Z. Yang, R. Ching, G. Trojandt, F. Odobel, *J. Am. Chem. Soc.* **1998**, *120*, 3536–3537. (b) D. Wilson, L. Perlson, R. Breslow, *Bioorg. Med. Chem.* **2003**, *11*, 2649–2653. (c) Y. Liu, G.-S. Chen, Y. Chen, F. Ding, T. Liu, Y.-L. Zhao, *Bioconjugate Chem.* **2004**, *15*, 300–306.

8 For reviews: (a) M. M. Conn, J. Rebek, Jr., *Chem. Rev.* **1997**, *97*, 1647–1668. (b) S. Leininger, B. Olenyuk, P. J. Stang, *Chem. Rev.* **2000**, *100*, 853–908. (c) D. M. Vriezema, M. C. Aragonès, J. A. A. W. Elemans, J. J. L. M. Cornelissen, A. E. Rowan, R. J. M. Nolte, *Chem. Rev.* **2005**, *105*, 1445–1489.

9 (a) L. R. MacGillivray, J. L. Atwood, *Nature*, **1997**, *389*, 469–472. (b) A. Shivanyuk, J. Rebek, Jr., *Proc. Natl. Acad. Sci. USA* **2001**, *98*, 7662–7665. (c) G. W. V. Cave, J. Antesberger, L. J. Barbour, R. M. McKinlay, J. L. Atwood, *Angew. Chem.* **2004**, *116*, 5375–5378. *Angew. Chem. Int. Ed.* **2004**, *43*, 5263–5266.

10 (a) L. Trembleau, J. Rebek, Jr., *Science* **2003**, *301*, 1219–1220. (b) A. Scarso, L. Trembleau, J. Rebek, Jr., *Angew. Chem.* **2003**, *115*, 5657–5660. *Angew. Chem. Int. Ed.* **2003**, *42*, 5499–5502.

11 (a) M. Fujita, K. Umemoto, M. Yoshizawa, N. Fujita, T. Kusukawa, K. Biradha, *Chem. Commun.* **2001**, 509–518. (b) M. Tominaga, K. Suzuki, M. Kawano, T. Kusukawa, T. Ozeki, S. Sakamoto, K. Yamaguchi, M. Fujita, *Angew. Chem.* **2004**, *116*, 5739–5743. *Angew. Chem. Int. Ed.* **2004**, *43*, 5621–5625. (c) K. Kumazawa, Y. Yamanoi, M. Yoshizawa, T. Kusukawa, M. Fujita, *Angew. Chem.* **2004**, *116*, 6062–6066. *Angew.*

Chem. Int. Ed. **2004**, *43*, 5936–5940. (d) T. Yamaguchi, S. Tashiro, M. Tominaga, M. Kawano, T. Ozeki, M. Fujita, *J. Am. Chem. Soc.* **2004**, *126*, 10818–10819. (e) M. Yoshizawa, J. Nakagawa, K. Kumazawa, M. Nagao, M. Kawano, T. Ozeki, M. Fujita, *Angew. Chem.* **2005**, *117*, 1844–1847. *Angew. Chem. Int. Ed.* **2005**, *44*, 1810–1813.

12 (a) D. L. Caulder, K. N. Raymond, *Acc. Chem. Res.* **1999**, *32*, 975–982. (b) P. N. W. Baxter, J.-M. Lehn, B. O. Kneisel, G. Baum, D. Fenske, *Chem. Eur. J.* **1999**, *5*, 113–120. (c) S. R. Seidel, P. J. Stang, *Acc. Chem. Res.* **2002**, *35*, 972–983.

13 (a) M. Fujita, D. Oguro, M. Miyazawa, H. Oka, K. Yamaguchi, K. Ogura, *Nature* **1995**, *378*, 469–471. (b) T. Kusukawa, M. Fujita, *J. Am. Chem. Soc.* **1999**, *121*, 1397–1398. (c) M. Yoshizawa, T. Kusukawa, M. Fujita, K. Yamaguchi, *J. Am. Chem. Soc.* **2000**, *122*, 6311–6312. (d) M. Yoshizawa, Y. Takeyama, T. Okano, M. Fujita, *J. Am. Chem. Soc.* **2003**, *125*, 3243–3247. (e) M. Yoshizawa, M. Tamura, M. Fujita, *J. Am. Chem. Soc.* **2004**, *126*, 6846–6847. (f) K. Nakabayashi, M. Kawano, M. Yoshizawa, S. Ohkoshi, M. Fujita, *J. Am. Chem. Soc.* **2004**, *126*, 16694–16695. (g) M. Yoshizawa, T. Kusukawa, M. Kawano, T. Ohhara, I. Tanaka, K. Kurihara, N. Niimura, M. Fujita, *J. Am. Chem. Soc.* **2005**, *127*, 2798–2799. (h) S. Tashiro, M. Tominaga, M. Kawano, B. Therrien, T. Ozeki, M. Fujita, *J. Am. Chem. Soc.* **2005**, *127*, 4546–4547.

14 (a) M. Fujita, S.-Y. Yu, T. Kusukawa, H. Funaki, K. Ogura, K. Yamaguchi, *Angew. Chem.* **1998**, *110*, 2192–2196. *Angew. Chem. Int. Ed.* **1998**, *37*, 2082–2085. (b) S.-Y. Yu, T. Kusukawa, K. Biradha, M. Fujita, *J. Am. Chem. Soc.* **2000**, *122*, 2665–2666. (c) M. Yoshizawa, T. Kusukawa, M. Fujita, S. Sakamoto, K. Yamaguchi, *J. Am. Chem. Soc.* **2001**, *123*, 10454–10459..

15 (a) P. Job, *Compt. Rend.* **1925**, *180*, 928. (b) W. Likussar, D. F. Boltz, *Anal. Chem.* **1971**, *43*, 1265–1272.

16 M. Fujita, F. Ibukuro, H. Hagihara, K. Ogura, *Nature*, **1994**, *367*, 720–723.

17 K. Wüthrich, *NMR of Proteins and Nucleic Acids*, Wiley, New York, **1986**.

18 (a) B. Hasenknopf, J.-M. Lehn, N. Boumediene, A. Dupont-Gervais, A. V. Dorsselaer, B. Kneisel, D. Fenske, *J. Am. Chem. Soc.* **1997**, *119*, 10956–10962. (b) M. Scherer, D. L. Caulder, D. W. Johnson, K. N. Raymond, *Angew. Chem.* **1999**, *111*, 1690–1694. *Angew. Chem. Int. Ed.* **1999**, *38*, 1588–1592. (c) S. Otto, R. L. E. Furlan, J. K. M. Sanders, *Science* **2002**, *297*, 590–593. (d) Y. Kubota, S. Sakamoto, K. Yamaguchi, M. Fujita, *Proc. Natl. Acad. Sci. USA* **2002**, *99*, 4854–4856. (e) S. Hiraoka, K. Harano, M. Shiro, M. Shionoya, *Angew. Chem.* **2005**, *117*, 2787–2791. *Angew. Chem. Int. Ed.* **2005**, *44*, 2727–2731.

Chapter 6

Folding of Ala-Ala-Ala Tripeptide into a Minimal Helix via Hydrophobic Encapsulation

Abstract

A tripeptide Ac-Ala-Ala-Ala-NH_2 folded into minimal helix, namely β-turn structure in water through hydrophobic binding within a self-assembled porphyrin cage. The turn conformation of the bound peptide was fully assigned from NOESY measurements, and strongly supported by molecular dynamics simulations. From single mutation experiments and molecular modeling, CH-π interactions between methyl groups of Ala residues and porphyrin ligands seem to be important in stabilization of the turn conformation. Furthermore, we observed the highly site-selective encapsulation of heptapeptide, Ac-Gly-Gly-Ala-Ala-Ala-Gly-Gly-NH_2, possessing Ala-Ala-Ala turn region at middle position.

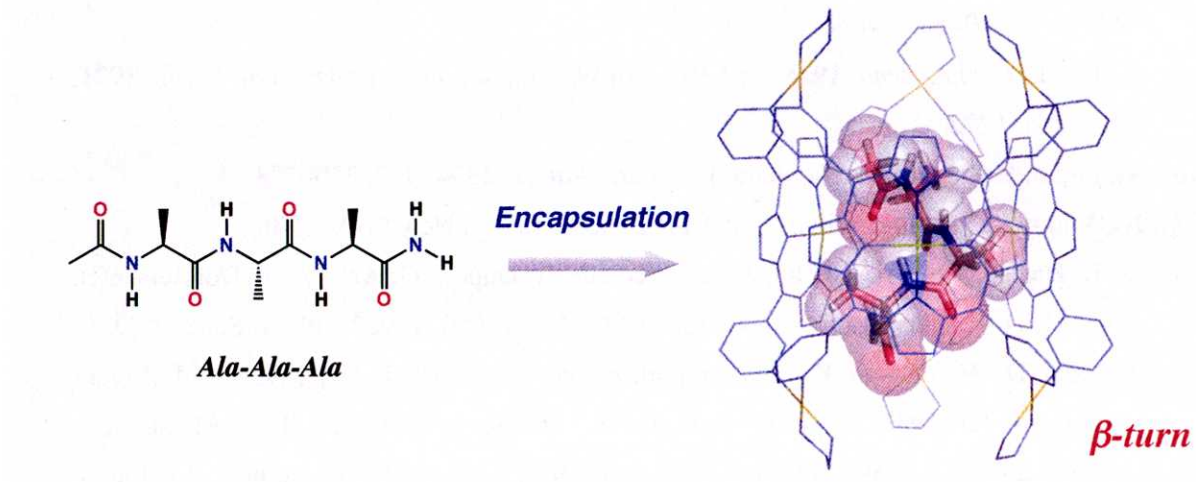

6.1 Introduction

While helical conformation is one of the most important secondary structures of peptides, this fundamental motif is, like other peptide secondary structures, very unstable if a peptide exists as a short fragment.[1] A minimal 3_{10}-helix can be, in principle, constituted by four amino acid residues via hydrogen bonding between C*O*(*i*) and N*H*(*i*+3). In general, however, at least 15 amino acid residues are required to form a stable helical conformation in water unless the helix is fixed by covalent or coordination bonds.[2,3,4] Here, we observe that even a three-residue peptide fragment, Ac-Ala-Ala-Ala-NH_2, can be folded into a minimal 3_{10}-helix (which is also categorized as β-turn[5]) through encapsulation by a porphyrin-assembled synthetic host. Despite the presence of only one intramolecular hydrogen bond, the minimal helix is shown to be very stable because of efficient host-guest interaction.

6.2 Results and Discussion

6.2.1 Strategy for the stabilization of short turn structure

For the efficient accommodation of a short peptide fragment, we employed prism-like porphyrin cage **1**[6] that provides a large hydrophobic binding pocket. This cage can be prepared by the self-assembly of tetrakis(3-pyridyl) substituted porphyrin and (en)Pd(NO_3)$_2$. The target tripeptide, Ac-Ala-Ala-Ala-NH_2 (**2**), contains only Ala that is the simplest α-substituted amino acid residue with propensity for α-helical conformation.[7]

6.2.2 ^{1}H NMR studies of complexation of **1** and **2**

The complex **1•2** was easily prepared by mixing the aqueous solutions of the both components ([**1**] = [**2**] = 2 mM) at room temperature for a few minutes. Encapsulation of **2** within the cavity of **1** was confirmed by ^{1}H NMR analysis. Proton signals of complexed **2** were fully assigned from TOCSY and NOESY experiments. All the signals of **2** were considerably shifted up-field. In particular, the Hβ protons of Ala1, Ala2, and Ala3 were observed around –5.0 ppm (Figure 1). This result suggested that all residues of peptide **2** were deeply encapsulated by the cavity of **1**. The association constant was estimated to be 1 x 10^6 M^{-1} by ^{1}H NMR competition experiment.[8]

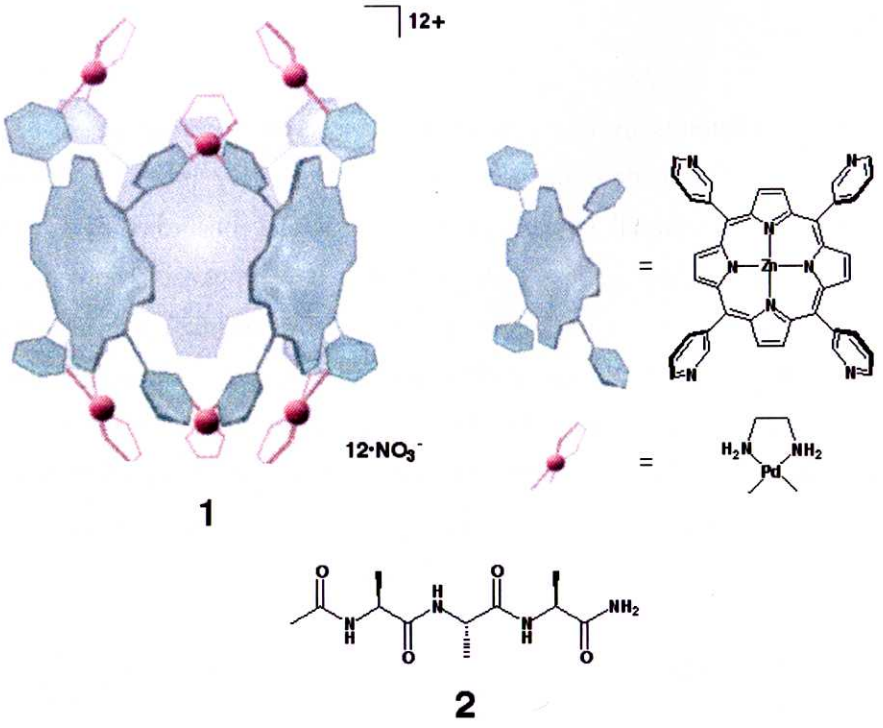

6.2.2 ^{1}H NMR studies of complexation of **1** and **2**

The complex **1•2** were easily prepared by mixing of both aqueous solutions ([**1**] = [**2**] = 2 mM) at room temperature for a few minutes. Encapsulation of **2** within the cavity of **1** was confirmed by ^{1}H NMR analysis. Proton signals of complexed **2** were assigned from TOCSY and NOESY experiments. Interestingly, all signals of **2** were highly up-field shifted, in particular, Hβ of Ala1, Ala2 and Ala3 were observed around –5.0 ppm (Figure 2). This result suggested that all residues of peptide **2** were perfectly encapsulated by the capsule-like cavity of **1**.

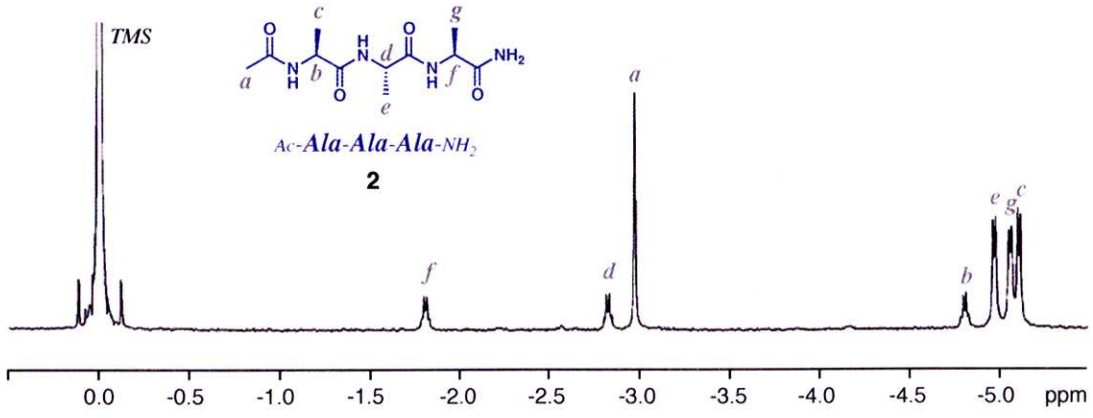

Figure 1. ^{1}H NMR spectrum of complex **1•2** in D_2O (500 MHz, 2 mM, 27 °C, TMS as external standard).

6.2.3 Conformation analysis of **2** within **1**

The turn conformation of **2** was elucidated from an NOESY experiment. NOE cross-peaks in NOESY were clearly observed between N-terminal acetyl group and Ala3 protons (HN and Hβ), indicating the proximity of the N- and C-terminal of **2** (Figure 2). The turn structure of **2** was also supported by $^3J_{NHCH\alpha}$coupling constants. All $^3J_{NHCH\alpha}$ values were below 6 Hz, being characteristic of helical rather than random-coil conformation.[9]

Furthermore, the turn structure was strongly suggested to be a minimal 3_{10}-helix conformation by molecular dynamics (MD) simulation with CNS program[10] that run under restraints of NOE distances (11 intra-residue, 7 sequential, 5 medium-range) and 3 backbone ϕ angles from $^3J_{NHCH\alpha}$ values. Among randomly generated 50 initial structures, 48 of them were converged, with low backbone pairwise RMSD (0.09 Å), into almost identical lowest-energy structures that clearly showed the turn conformation (Figure 3). The MD calculation also suggested a hydrogen bond between N-terminal acetyl group and NH of Ala3. This turn structure is a minimal 3_{10}-helix and also categorized as β-turn conformation.[11]

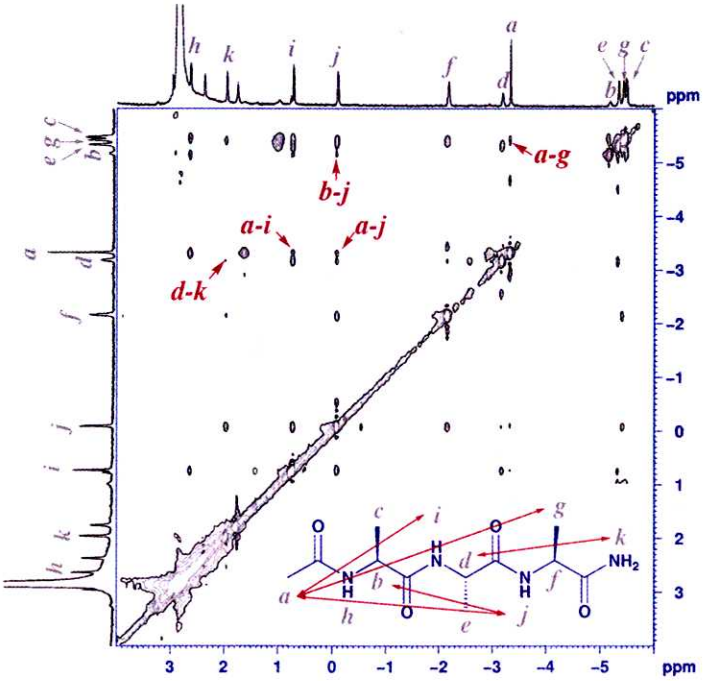

Figure 2. Selected NOESY spectrum (500 MHz, H_2O/D_2O = 9/1, 27 °C) of **1** ([**1**] = 2 mM) and **2** ([**2**] = 2 mM). Inter-residue NOEs are denoted as alphabet in spectrum and as arrows in chemical structure of **2**.

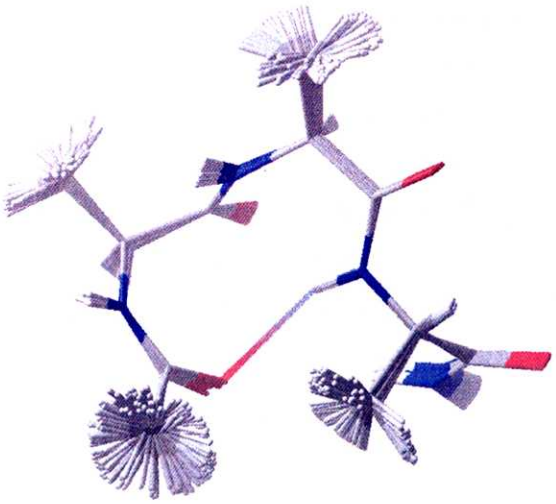

Figure 3. Superposition of the 48 lowest energy structures by CNS[10] for bound peptide **2**.

6.2.4 Validity of the turn structure of **2** by molecular modeling

We confirmed that the MD minimized structure fits the cavity of **1**. The crystal structure of **1**[6] and the MD optimized structure of **2** were combined so that **2** was fully accommodated in the cavity of **1**. When the combined structure was refined,[12] the conformation of **2** remained almost unchanged, suggesting that host **1** provides an ideal cavity for recognizing the most stable conformation of **2** (Figure 4). For comparison, tripeptide **2** in an extended conformation was also refined in the cavity of **1**, but efficient host-guest interactions were hardly observed.

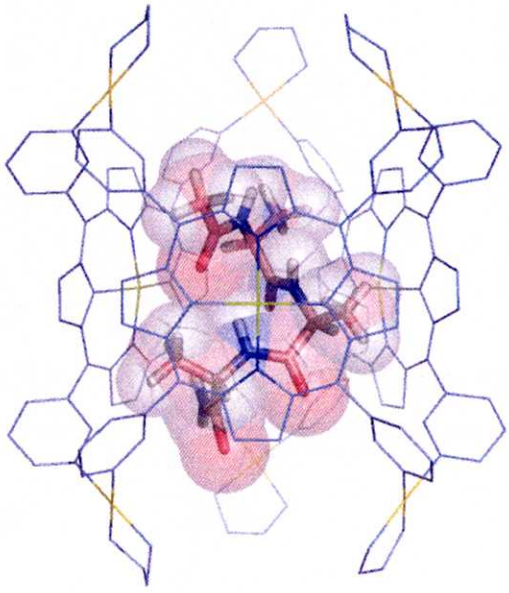

Figure 4. Refined structure of the complex **1**•**2**[12] from crystal structure of **1** and MD minimized structure of **2**.

6.2.5 Sequence-selective recognition of aliphatic tri-peptide by the porphyrin capsule 1

In the refined **1•2** structure, the methyl groups of Ala residues and the porphyrin ligands showed efficient CH-π contact, which presumably induces the folding of **2** into the minimal helix conformation. In particular, the CH-π contact of Ala2 seems the most important because the association constant of **1** with a singly Gly-mutated tripeptide, Ac-Ala-*Gly*-Ala-NH_2 (**3**), was considerably reduced (9 x 10^3 M^{-1}) (Table 1). Other Gly-mutated tripeptides, Ac-*Gly*-Ala-Ala-NH_2 (**4**) and Ac-Ala-Ala-*Gly*-NH_2 (**5**), did not show significant decrease in association constants (8 x 10^5 and 1 x 10^6 M^{-1} for **4** and **5**, respectively). Binding was no longer observed for Ac-Gly-Gly-Gly-NH_2 (**6**) because of the absence of the CH-π contact. Tripeptides, Ac-Val-Val-Val-NH_2 (**7**) and Ac-Leu-Leu-Leu-NH_2 (**8**), were also not bound at all because they are too bulky to be fit in the cavity of **1**.

Table 1. Association constants of **1** with aliphatic tri-peptides in water

Peptides	K_a (M^{-1})
Ac-**Ala**-**Ala**-**Ala**-NH_2 (**2**)[a]	1 x 10^6
Ac-**Ala**-Gly-**Ala**-NH_2 (**3**)[b]	9 x 10^3
Ac-Gly-**Ala**-**Ala**-NH_2 (**4**)[b]	8 x 10^5
Ac-**Ala**-**Ala**-Gly-NH_2 (**5**)[b]	1 x 10^6
Ac-Gly-Gly-Gly-NH_2 (**6**)	no binding
Ac-Val-Val-Val-NH_2 (**7**)	no binding
Ac-Leu-Leu-Leu-NH_2 (**8**)	no binding

[a] Measured by NMR competition experiment with Ac-Trp-Trp-Ala-NH_2. [b] Measured by NMR competition experiment with **2**.

6.2.6 Selective recognition of Ala-Ala-Ala sequence within the porphyrin capsule 1

Particularly interesting is that, through host-guest interaction with **1**, a stable turn structure seem to be generated from a longer oligopeptide involving Ala-Ala-Ala sequence in the middle. When a heptapeptide, Ac-Gly-Gly-Ala-Ala-Ala-Gly-Gly-NH_2 (**9**), was treated with an equiv molar of **1** in water, significant upfield shifts of proton signals were observed only at the Ala-Ala-Ala region ($\Delta\delta$ = 5.6, 6.3, and 6.6 ppm for the methyl groups of Ala3, Ala4, and Ala5, respectively). The adjacent Gly2 and Gly6 were also shifted upfield ($\Delta\delta$ = 6 and 4 ppm for the methylene groups of Gly2 and Gly6, respectively), while terminal Ac-Gly1 and Gly7-NH_2 protons were hardly shielded (Figure 5). Even in longer peptide, Ala-Ala-Ala sequence was selectively accommodated in the cavity.

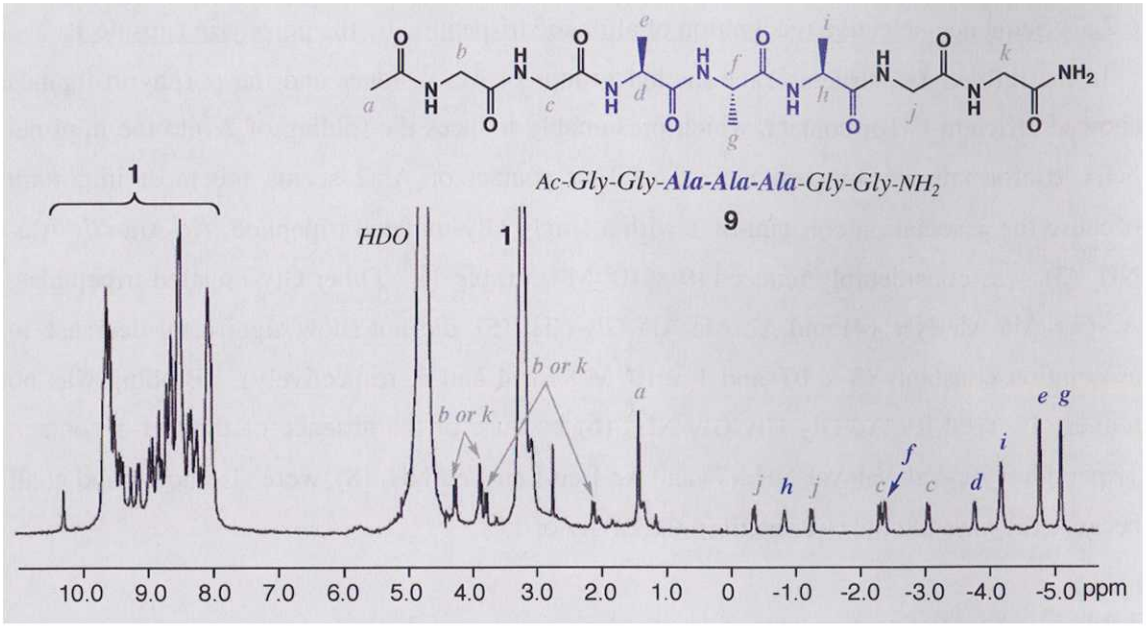

Figure 5. ^{1}H NMR spectrum of complex **1•9** in D_2O (500 MHz, 2 mM, 27 °C).

6.3 Conclusion

In conclusion, self-assembled porphyrin cage **1** showed remarkable ability to bind and fold Ala-Ala-Ala sequence into a minimal helix or β-turn. The result demonstrated that peptide recognition within a large cavity of self-assembled cages is a powerful method to produce the secondary structures of peptides even if the peptide fragment is considerably short.

6.4 Experimental Section

Peptide synthesis, procedure of UV titration, NMR measurements, competition experiment and structural calculations by CNS were described in General Experimental Section. The porphyrin cage **1** was prepared following procedure as reported earlier.[6]

Structure refinement by MacroModel 8.0

The coordinate of **1** from X-ray structure[6] was fixed, and only peptide structure, whose initial coordinate was calculated structure by CNS, was refined in **1** by using the OPLS-AA force field in MacroModel 8.0 (Schrödinger, Inc.).

Physical data of 1•2

^{1}H NMR (500 MHz, D_2O, 27 °C, TMS as external standard): δ 9.59 (br, 16H, **1**), δ 9.00-8.38 (br, 16H, **1**), δ 8.30-7.80 (br, 32H, **1**), δ 3.23 (br, 24H, **1**), δ -1.80 (q, *J* = 7.3 Hz, 1H, **2**), δ -2.81 (q, *J* = 7.3 Hz, 1H, **2**), δ -2.96 (q, *J* = 7.3 Hz, 3H, **2**), δ -4.79 (q, *J* = 7.3 Hz, 1H, **2**), δ -4.96 (d, *J* = 7.3 Hz, 3H, **2**), δ -5.06 (d, *J* = 7.3 Hz, 3H, **2**), δ -5.09 (d, *J* = 7.3 Hz, 3H, **2**).

^{13}C NMR (125 MHz, D_2O, 27 °C, TMS as external standard): δ 180-160 (*C*O x4, **2**), δ 151.9–149.9 (*C*H, **1**), δ 147.2–145.3 (*C*H, **1**), δ 141.8–141.2 (*C*q, **1**), δ 133.1–130.9 (*C*H, **1**), δ 126.4–124.4 (*C*H, **1**), δ 115.0–113.5 (*C*q, **1**), δ 47.1 (*C*H_2, **1**), δ 45.4 (*C*H, **2**), δ 45.3 (*C*H, **2**), δ 45.0 (*C*H, **2**), δ 15.8 (*C*H_3, **2**), δ 10.8 (*C*H_3, **2**), δ 10.7 (*C*H_3, **2**), δ 10.2 (*C*H_3, **2**).

IR (KBr, cm^{-1}): 1653.2, 1522.6, 1475.5, 1384.5, 1191.8, 1056.0, 1036.0, 994.5, 796.6, 698.0.

6.5 References

1 B. H. Zimm, J. K. Bragg, *J. Chem. Phys.* **1959**, *31*, 526–535.

2 Covalent bonding: (a) D. Y. Jackson, D. S. King, J. Chmielewski, S. Singh, P. G. Schultz, *J. Am. Chem. Soc.* **1991**, *113*, 9391–9392. (b) C. Bracken, J. Gulyás, J. W. Taylor, J. Baum, *J. Am. Chem. Soc.* **1994**, *116*, 6431–6432. (c) E. Cabezas, A. C. Satterthwait, *J. Am. Chem. Soc.* **1999**, *121*, 3862–3875. (d) C. E. Schafmeister, J. Po, G. L. Verdine, *J. Am. Chem. Soc.* **2000**, *122*, 5891–5892. (e) R. N. Chapman, G. Dimartino, P. S. Arora, *J. Am. Chem. Soc.* **2004**, *126*, 12252–12253.

3 Metal coordination: (a) M. R. Ghadiri, C. Choi, *J. Am. Chem. Soc.* **1990**, *112*, 1630–1632. (b) F. Ruan, Y. Chen, P. B. Hopkins, *J. Am. Chem. Soc.* **1990**, *112*, 9403–9404. (c) M. J. Kelso, H. N. Hoang, W. Oliver, N. Sakolenko, D. R. March, T. G. Appleton, D. P. Fairlie, *Angew. Chem. Int. Ed.* **2003**, *42*, 421–424. (d) A. Ojida, M. Inoue, Y. Mito-oka, I. Hamachi, *J. Am. Chem. Soc.* **2003**, *125*, 10184–10185.

4 Other interactions: (a) M. W. Peczuh, A. D. Hamilton, J. Sánchez-Quesada, J. de Mendoza, T. Haack, E. Giralt, *J. Am. Chem. Soc.* **1997**, *119*, 9327–9328. (b) Y. Inai, K. Tagawa, A. Takasu, T. Hirabayashi, T. Oshikawa, M. Yamashita, *J. Am. Chem. Soc.* **2000**, *122*, 11731–11732. (c) D. Wilson, L. Perlson, R. Breslow, *Bioorg. Med. Chem.* **2003**, *11*, 2649–2653. (d) A. Verma, H. Nakade, J. M. Simard, V. M. Rotello, *J. Am. Chem. Soc.* **2004**, *126*, 10806–10807.

5 For reviews on β-turn mimetic: (a) A. Giannis, T. Kolter, *Angew. Chem. Int. Ed. Engl.* **1993**, *32*, 1244–1267. (b) J. P. Schneider, J. W. Kelly, *Chem. Rev.* **1995**, *95*, 2169–2187. (c) S. Hanessian, G. McNaughton-Smith, H.-G. Lombart, W. D. Lubell, *Tetrahedron*, **1997**,

53, 12789–12854. (d) K. D. Stigers, M. J. Soth, J. S. Nowick, *Curr. Opin. Chem. Biol.* **1999**, *3*, 714–723. (e) K. Burgess, *Acc. Chem. Res.* **2001**, *34*, 826–835.

6 N. Fujita, K. Biradha, M. Fujita, S. Sakamoto, K. Yamaguchi, *Angew. Chem. Int. Ed.* **2001**, *40*, 1718–1721.

7 P. C. Lyu, M. I. Liff, L. A. Marky, N. R. Kallenbach, *Science* **1990**, *250*, 669–673.

8 The association constant for **1•2** complex could not be directly determined by titration abecause of little change in absorbance and fluorescence on complexation. Thus the association constant of an aromatic tripeptide was measured by UV-titration. Then, the association constant for **1•2** was estimated by an NMR competition experiment with the aromatic peptide.

9 H. J. Dyson, P. E. Wright, *Annu. Rev. Biophys. Biophys. Chem.* **1991**, *20*, 519–538.

10 A. T. Brünger, P. D. Adams, G. M. Clore, W. L. DeLano, P. Gros, R. W. Grosse-kunstleve, J.-S. Jiang, J. Kuszewski, M. Nilges, N. S. Pannu, R. J. Read, L. M. Rice, T. Simonson, G. L. Warren, *Acta Crystallogr. Sect. A* **1998**, *54*, 905–921.

11 Calculated structure by CNS was exactly categorized as β-turn type I.

12 Structure refinements were carried out using MacroModel 8.0 and the OPLS-AA force field.

Chapter 7

Toward Dynamic Peptide Receptors: Control of Dynamic Aspect of Guest Molecules within Tubular Receptor

Abstract

Rod-like guests accommodated in self-assembled coordination nanotubes are shown to stay in the tubes without flipping along its length at room temperature, but rapidly exchange intermolecularly at high temperature.

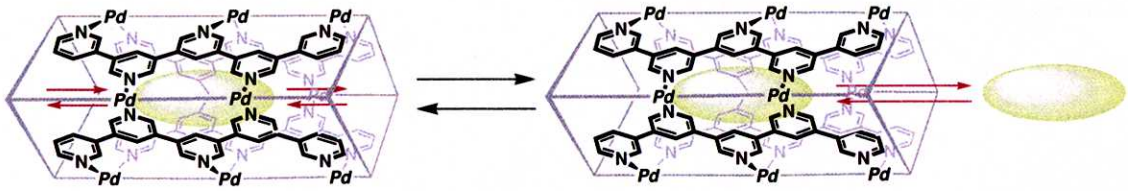

7.1 Introduction

We considered that ideal peptide recognitions are not only the stabilization of static peptide conformation, but also a control of peptide dynamics. For the controlling of such dynamics, guest molecule needs to be accommodated in much restricted cavities. For example, guest molecule in tubular cavity is allowed only one-dimensional motion. Therefore, fundamental study of guest dynamics in such a tubular cavities is expected to be useful to the rational design of novel artificial peptide receptors which can regulate the peptide dynamics.

Oligo(3,5-pyridine) ligands **1** have been shown to self-assemble into coordination nanotubes **2** in the presence of rod-like guests.[1] The previous paper has described that the rod-like guests take an important role to template the assembly of the tubes and to stabilize the tubular structures. Studies on the dynamic behavior of the guest molecules that are accommodated in the tubes are particularly interesting due to the novel functions of tubular molecules: *e.g.* shape-selective transportation,[2] site-specific chemical transformation[3] and molecular level data storage.[4] Here we discuss the dynamic aspects of the host-guest complexation within the self-assembled coordination nanotubes.[5] NMR studies show that guests stay in the tubes without flipping along the length at room temperature, but rapidly exchange intermolecularly at high temperature.

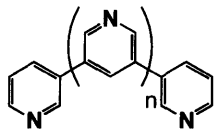

1 (**a**: n= 3, **b**: n= 1)

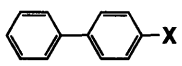

3a: X= COO^-
3b: X= CH_3

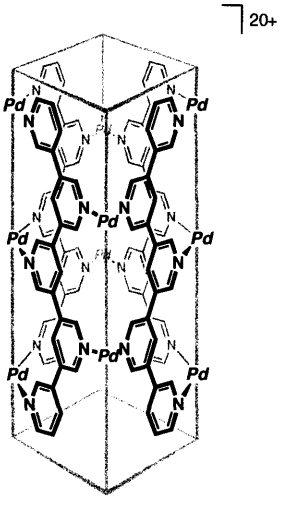

2a

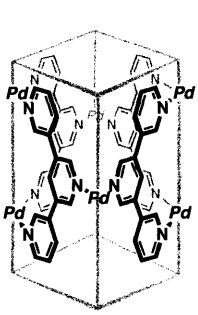

2b

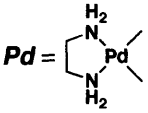

7.2 Result and Discussion

7.2.1 VT-NMR studies of guest dynamics in tubular complex

To address the guest motion in the tube, unsymmetrical biphenyl derivative **3a** was used as a template. Thus, (en)Pd(NO_3)$_2$, ligand **1a** and Na^+•**3a** were combined at a ratio of 10:4:1 in D_2O. After 1 h at 70 °C, NMR revealed the self-assembly of tube **2a•3a**. Guest signals were upfield shifted and observed at δ 5.2–5.5 indicating the efficient accommodation of **3a** in nanotube **2a**.

A significant observation by NMR is the dissymmetrization of the host framework at ambient temperature: *e.g.* H*d* ≠ H*d'* and H*e* ≠ H*e'* as shown in Figure 1a. Upon heating, these couples coalesced at 47 °C (Figure 1b and c).[6] These results evidence the following guest behaviors: (i) the guest molecule is trapped in the tube and unable to flip at room temperature on the NMR timescale, dissymmetrizing the host framework. (ii) the guest spins around its long axis because all four units of **1a** in the tube are found equivalent in the NMR spectrum. (iii) at high temperature, the guest got an opportunity to be released from the tube, symmetrizing the host environment.

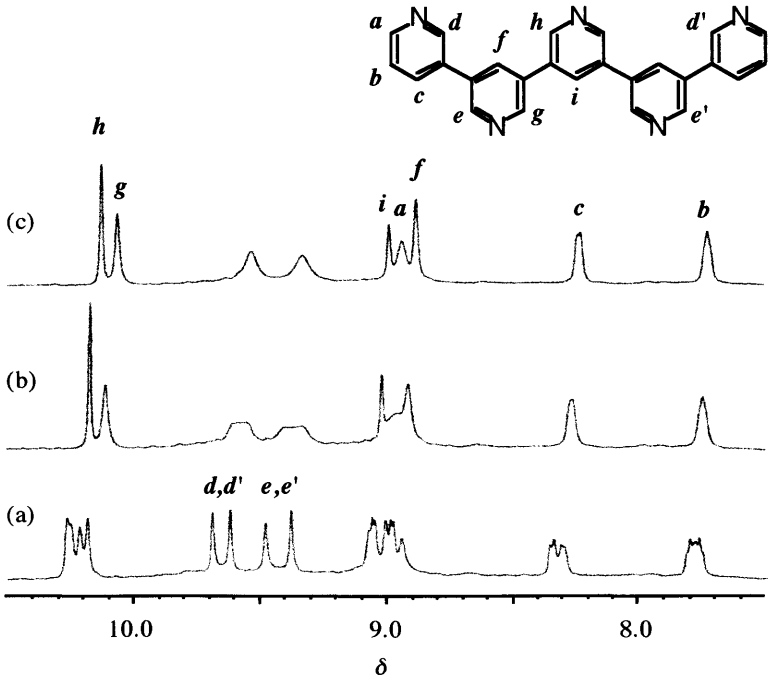

Figure. 1 Variable-temperature ^{1}H NMR spectra of **2a•3a** recorded in D_2O at (a) 27 °C, (b) 47 °C and (c) 60 °C (500 MHz, TMS as an external standard).

7.2.2 Effect of the excess guest molecules for the bound guest dynamics

The coalescence temperature *Tc* (47 °C) markedly changed upon the addition of excess amount of the guest. For example, when small amount (0.1 equiv.) of the guest was added to the 1:1 host–guest complex, *Tc* was dramatically dropped to 33 °C as revealed by VT NMR measurement. Further addition of the guest (up to 2.0 equiv.) caused gradual decrease in *Tc*: at [H]:[G] = 1:1.2 and 1:1.5, *Tc* was 29 and 14 °C, respectively. At [H]:[G] = 1:2, the dissymmetrization of the ligand framework was not observed even at 5 °C.

The significant change in *Tc* at [G]/[H] = 1 strongly suggests two possible pathways for guest release. When [G]/[H] < 1, guest molecules must self-dissociate via an empty intermediate (S_N1-like pathway, Figure 2a). In case of [G]/[H] > 1, guest can be replaced by the second guest via S_N2-like pathway (Figure 2b). Obviously, the latter process requires lower energy and, therefore, *Tc* is significantly dropped at [G]/[H] > 1. Since the S_N2-like displacement is accelerated with the increase of the guest concentration, *Tc* is gradually dropped upon the addition of further amount of the guest.

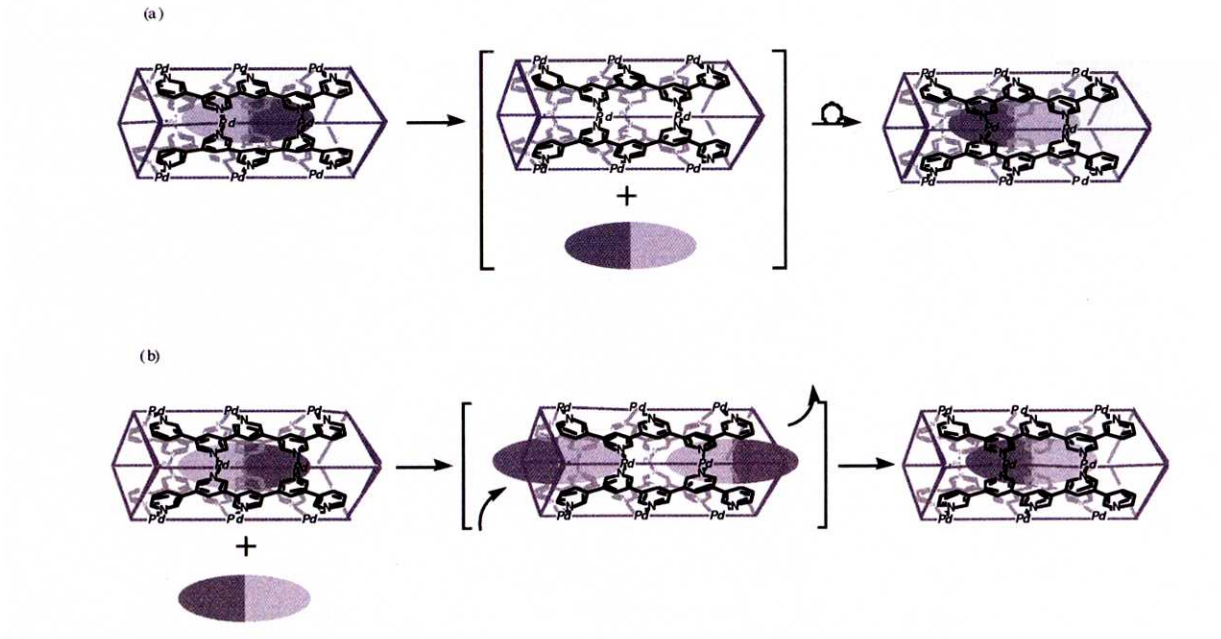

Figure. 2 Illustration for the mechanism of guest exchange at (a) [H]:[G] = 1:1 and (b) [H]:[G] = 1:2.

7.2.3 Host-guest stability depending on the tube length and nature of the guest molecules

Tc also depends on the tube length: when shorter tube **2b** was complexed with **3a** (1 equiv.), the host was symmetrized at *Tc* = 29 °C. Thus, the shorter tube can trap the guest less tightly.

The preferential binding of anionic guest **3a** over a neutral guest, 4-methylbiphenyl (**3b**), was shown by a guest exchange experiment. Thus, **2a•3b** complex was prepared by treating (en)Pd(NO_3)$_2$ with ligand **1a** in the presence of **3b** (D_2O, 20 h, 70 °C). Again, the dissymmetrization of the host framework was observed showing that this guest was also trapped in the tube at room temperature. Upon the addition of **3a** (1.0 equiv.) to this solution, however, guest **3b** was immediately replaced by **3a**. This result suggested that, in addition to the aromatic interactions, efficient electrostatic interaction between the tube and the template was also particularly important for the host-guest complexation.[1] The weaker host-guest interaction in **2a•3b** complex agreed well with its lower *Tc* value (29 °C) than that of **2a•3a** by 18 °C.

7.3 Conclusion

In conclusion, we revealed the one-dimensional motion of rod-like guest molecule in coordination tube complex **2**. The dynamic aspect of the guest molecule can be evaluated from VT-NMR measurements. The one-dimensional motion of guest can be also controlled by addition of excess guest molecules. This study is expected to be applicable to the rational design of novel artificial peptide receptors which can regulate the peptide dynamics.

7.4 Experimental Section

Materials and NMR measurements were described in General Experimental Section.

Preparation of 2a•3a

(en)Pd(NO_3)$_2$ (0.10 mmol) and **1a** (0.04 mmol) were combined in D_2O (2.0 mL) and stirred for 5 h at 70 °C. To this solution, an aqueous solution (0.1 mL) of Na^+•**3a** (0.01 mmol) was added and the mixture was stirred at 70 °C for 1 h.

7.5 References

1 M. Aoyagi, K. Biradha, M. Fujita, *J. Am. Chem. Soc.*, **1999**, *121*, 7457. Also see the preceding paper.

2 (a) M. R. Ghadiri, J. R. Granja, R. A. Milligan, D. E. McRee, N. Khazanovich, *Nature*, **1993**, *366*, 324. (b) M. Engels, D. Bashford, M. R. Ghadiri, *J. Am. Chem. Soc.*, **1995**, *117*, 9151. (c) J. Santamaria, T. Martin, G. Hilmersson, S. L. Craig, J. Rebek, Jr., *Proc. Natl. Acad. Sci. USA*, **1999**, *96*, 8344.

3 (a) A. Harada, J. Li, M. Kamachi, *Nature*, **1992**, *356*, 325. (b) A. Harada, J. Li, M. Kamachi, *Nature*, **1993**, *364*, 516.

4 (a) P.-L. Anelli, M. Asakawa, P. R. Ashton, R. A. Bissell, G. Clavier, R. Gorski, A. E. Kaifer, S. J. Langford, G. Mattersteig, S. Menzer, D. Philip, A. M. Z. Slawin, N. Spencer, J. F. Stoddart, M. S. Tolley, D. J. Williams, *Chem. Eur. J.*, **1997**, *3*, 1113. (b) A. C. Benniston, *Chem. Soc. Rev.*, **1996**, *25*, 427. (c) A. S. Lane, D. A. Leigh, A. Murphy, *J. Am. Chem. Soc.*, **1997**, *119*, 11092.

5 (a) R. G. Chapman, G. Olovsson, J. Trotter, J. C. Sherman, *J. Am. Chem. Soc.*, **1998**, *120*, 6252. (b) S. Ma, D. M. Rudkevich, J. Rebek, Jr., *Angew. Chem., Int. Ed. Engl.*, **1999**, *38*, 2600. (c) P. Timmerman, W. Verboom, D. N. Reinhoudt, *Tetrahedron*, **1996**, *52*, 2663.

6 From *Tc*, rate constant and activation energy were estimated to be 77.4 s^{-1} and 16.0 kcal/mol, respectively. See: S. Braun, H.-O. Kalinowski and S. Berger, *100 and More Basic NMR Experiment*. VCH, Weinheim, 1996.

Chapter 8

Toward Dynamic Peptide Receptors: Dynamic Assembly of Dodecapyridine Ligand into End-Capped and 3.0 nm Tubes

Abstract

Mono end-capped coordination tube that assembles from dodecapyridine ligand and six Pd^{II} ions is sufficiently stable but is converted into a doubly composed open tube through crystallization. The open tube once formed does not come back to the capped tube. These results indicate that, despite the labile nature of Pd^{II}-pyridine coordination bonds, both structures are not in a rapid equilibrium and are kinetically trapped during self-assembly.

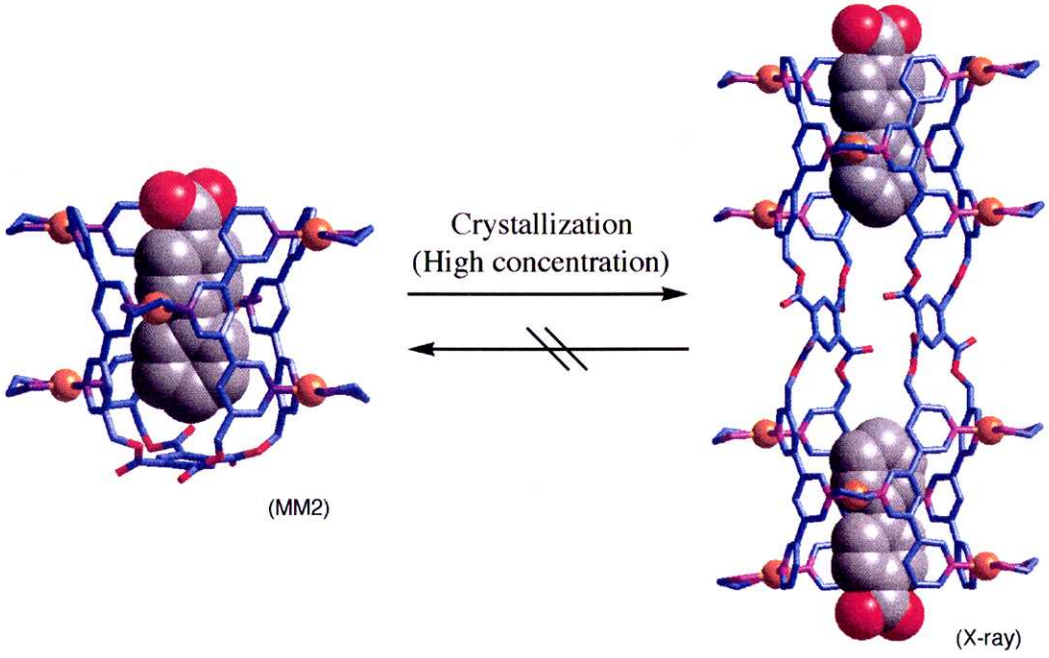

8.1 Introduction

We considered that one of the ideal peptide receptor is a dynamically self-assembled host molecules. Generally, these structures convert to other structures by external stimuli. Namely, if structure of peptide receptor can be regulated by external stimuli, we will control the peptide selectivity, peptide conformation in host, and catch/release of peptide, that is applicable to the drug delivery system, through structural transformation of receptors.

Dynamic assembly deals with two or more self-assemblies which are on a relatively flat potential energy surface and are interconverted to each other via resorting or reorganization of component species.[1-3] When dynamic structures have a cavity suitable for recognizing a guest, the predominant assembly of one particular host structure is induced by adding an appropriate guest. Such a guest-induced assembly of a specific host framework is often seen in biological events and has been actively studied both in hydrogen-bond and coordination assembly systems.[2] Here we report a unique dynamic assembly where, under a set of identical thermodynamic conditions, the same guest induces the formation of two different assemblies depending on whether the assembly process experiences crystallization or not.

The dynamic assembly discussed here stems from (en)Pd^{II} coordination block (**1**) and ligand **2** that has four tripyridine podands on a benzenetetracarboxylate scaffold.[4] On analogy to the guest-induced assembly of coordination nanotubes from oligo(3,5-pyridine) ligands and Pd units,[5] ligand **2** is expected to give mono end-capped coordination tube **3** upon complexation with **1** in the presence of an appropriate guest [Eq. (1a)].[6] This tube is designed to discriminate the both ends of symmetrical rod-like molecules. namely, one end accommodated at the bottom of the tube should show different properties from another end. We have found that, in addition to expected structure **3**, the complexation of **1** and **2** also gives rise to doubly composed open tube **4** in which ligand **2** adopts an extended conformation [Eq. (1b)]. This open tube is observed only at higher concentrations as a minor component, but isolated in a pure form through slow crystallization. Interestingly, once isolated **4** is not converted into **3** at lower concentrations, indicating that both structures are kinetically trapped at local minima of the potential surface. Accordingly, we discuss here the self-assembly and the host-guest behavior of end-capped tube **3** and open tube **4** as well as the importance of kinetic effects in their self-assembly processes.

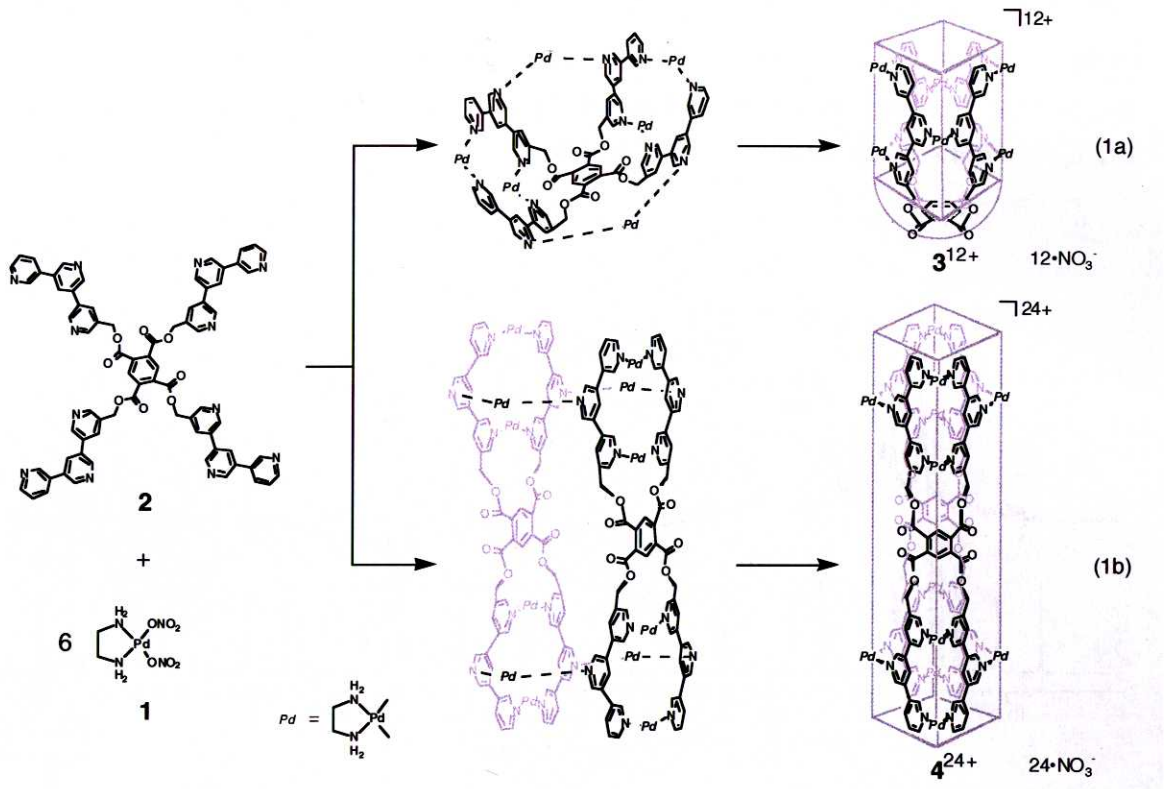

Scheme 1. Self-assemblies of mono end-capped tube **3** and doubly composed open tube **4**. For clarity, guest molecules are omitted.

8.2 Result and Discussion

8.2.1 Quantitative self-assembly of end-capped tube **3**

The quantitative assembly of **2** into end-capped tube **3** was, in fact, accomplished by the template effect of rod-like guests such as 4,4'-ditolyl (**5**). Without the template, the complexation of ligand **2** with (en)Pd(NO_3)$_2$ (**1**) in D_2O resulted in a complex mixture (Figure 1a). The addition of **5** to the solution, however, induced the assembly of a single product within 3 h at 70 °C (Figure 1b). In the tube structure, the side arms of **2** are equivalent whereas the methylene protons on each side arm are diastereotopic and thus observed as an AB quartet. In addition to satisfactory NMR, the formation of complex **3** was strongly supported by CSI-MS (coldspray-ionization mass spectrometry).[7,8]

^{1}H NMR observation featured some structural aspects of the inclusion complex. As expected, the two methyl groups of guest **5** accommodated in **3** were clearly discriminated being observed at δ -0.25 and 1.83 in NMR (Figure 1b). The significant upfield shift of one methyl (Δδ ca. -2.6 ppm from ordinary chemical shift) suggests that this methyl is located on

the benzene scaffold and surrounded by four side pyridine C rings. Below 60 °C, these two methyls were not coalesced indicating that the guest is strongly bound in the deep cavity of **5** and the flipping of the guest along its long axis is suppressed.[9] Aromatic protons of **5** were also upfield shifted being observed at δ 4.47–4.86.

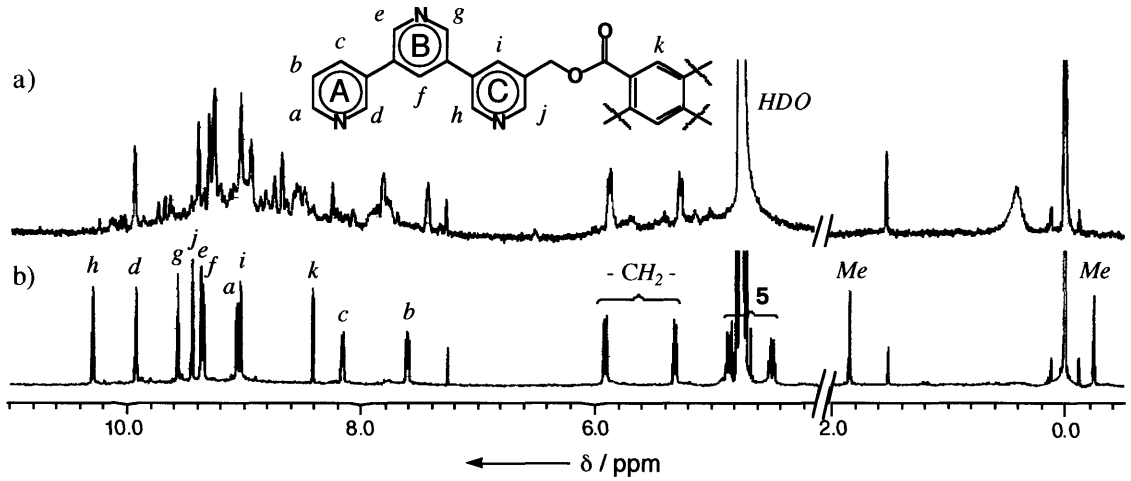

Figure 1. The ^{1}H NMR observation of the guest-templated formation of **5•3** (500 MHz, D_2O, 25 °C, TMS as an external standard). a) An oligomeric mixture obtained from **2** (1.7 μmol) and (en)Pd(NO_3)$_2$ (10.2 μmol) in D_2O (0.8 mL). b) **5•3** complex assembled upon the addition of **5** (1.7 μmol).

Asymmetric guest such as sodium biphenylcarboxylate (Na^+•**6**) was efficiently accommodated in a uni-directional fashion. Namely, only one isomer was formed in which the hydrophobic biphenyl group was deeply included in the tube and the hydrophilic carboxylate group was exposed outside as indicated by ^{1}H NMR (Figure 2a). Interestingly, disodium biphenyldicarboxylate ($2Na^+$•**7**), which was bound in an open tube in our previous study,[5] was not included in **3** showing that the end-capped site of **3** provides an efficient hydrophobic pocket that cannot bind the hydrophilic portion of the guest.

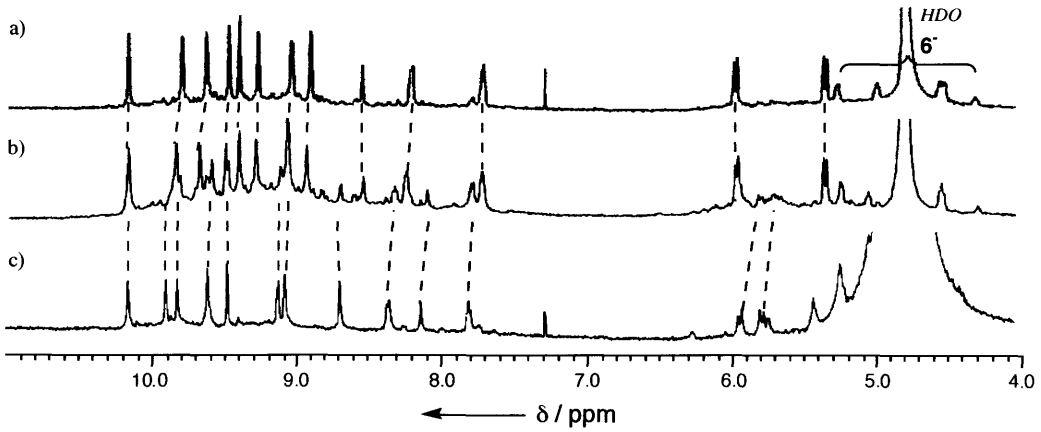

Figure 2. The ^{1}H NMR showing the conversion of **6•3** into $(\mathbf{6})_2$•**4** (500 MHz, D_2O, 25 °C, TMS as an external standard). a) $[\mathbf{2}]_0$ = 2.1 mM, b) $[\mathbf{2}]_0$ = 8.5 mM, c) complex $(\mathbf{6})_2$•**4** isolated as crystals.

8.2.2 Self-assembly of open tube **4** at high concentration

The self-assembly of inclusion complex **6•3** was concomitant with the formation of a minor component at high concentrations ($[\mathbf{2}]_0$ > 8 mM, Figure 2b). Fortunately, this minor product was isolated as single crystals by slow evaporation (> two weeks) of the solution. The X-ray crystallographic analysis showed that this product is a doubly composed open tube **4** consisting of two molecules of ligand **2** which are held together by twelve (en)Pd units (Figure 3). Open tube **4** accommodates two molecules of **6**, each of which is oriented so that its carboxylate group is exposed outside. An important feature is that the 16-component self-assembly (two ligands, twelve metals, and two guests) gives 3.0 nm molecular tube which is one of the longest among those structurally defined by crystallography. The biphenyl moiety is surrounded by hydrophobic framework through efficient π – π and CH– π interactions. The elemental analysis was consistent with a formula of $(Na^+\bullet\mathbf{6})_2\bullet\mathbf{4}\bullet(NO_3)_{24}\bullet45H_2O$.

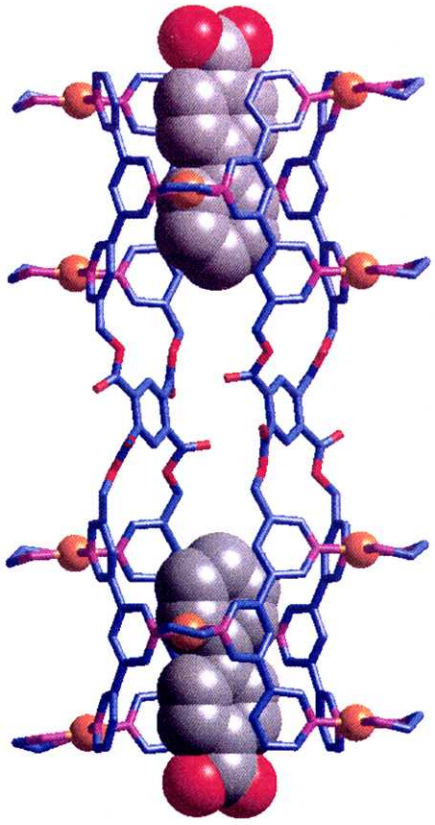

Figure 3. Crystal structure of $(\mathbf{6})_2$•**4**. For clarity, H atoms, water molecules, and NO_3^- ions are omitted.

8.2.3 Structural transformation from end-capped tube to open tube via crystallization

The stability of once isolated $(\mathbf{6})_2$•**4** complex deserves special attention. When the crystals of $(\mathbf{6})_2$•**4** were dissolved in D_2O at room temperature, we observed $(\mathbf{6})_2$•**4** complex in a pure form (Figure 2c) although **6**•**3** complex was the major product before isolation. More surprisingly, $(\mathbf{6})_2$•**4** complex remained unchanged in solution even after one month. These results clearly show that **6**•**3** and $(\mathbf{6})_2$•**4** complexes are not in equilibrium despite the labile nature of Pd^{II}-pyridine coordination bonds. Only at high concentrations for crystallization **6**•**3** is slowly converted into $(\mathbf{6})_2$•**4** complex.

It is noteworthy that, under a set of identical thermodynamic conditions, we obtained two different assemblies **6**•**3** and $(\mathbf{6})_2$•**4** depending on whether the assembly process includes crystallization or not. We thus suggest the followings: (i) **6**•**3** and $(\mathbf{6})_2$•**4** complexes, being sustained by 12 and 24 Pd^{II}-pyridine coordination bonds, respectively, are not thermodynamic but kinetically trapped structures. (ii) **6**•**3** complex is kinetically formed and trapped via intramolecular complexation although more stable $(\mathbf{6})_2$•**4** complex also exists on a potential

energy surface. (iii) the interconversion of **6•3** into $(\mathbf{6})_2$•**4** is substantially ignored at low concentrations, but slowly promoted at high concentrations, and much more facilitated by removing $(\mathbf{6})_2$•**4** complex by crystallization.

8.3 Conclusion

In conclusion, we observed dynamic self-assembly of two tubular structure, end-capped tube **3** and 3.0 nm open tube **4** from same ligand **2** and metal ion **1**. At low concentration, only end-capped tube **3** was formed. On the other hand, at higher concentration, two tubes were self-assembled as mixture. Crystallization accelerated the structural transformation from **3** to 3.0 nm open tube **4**. We considered that end-capped tube **3** is kinetically trapped structure, and open tube **4** is thermodynamically stable structure. This dynamic self-assembly is expected to be applied to the dynamic peptide receptor, because we can prepare various shaped receptors by the solution condition.

8.4 Experimental Section

Materials and NMR measurements were described in General Experimental Section.

Synthesis of Tetrakis(5-bromopyridin-3-ylmethyl) 1,2,4,5-benzenetetracarboxylate (10)

To a mixture of 5-bromo-3-hydroxymethylpyridine[10] (4.84 g, 25.7 mmol), pyromellitic acid (1.06 g, 4.16 mmol), and triphenylphosphine (10.90 g, 41.6 mmol) in dry THF (500 mL) cooled to 0 °C with an ice bath was added dropwise a solution of diethyl azodicarboxylate (62.4 mmol, 0.21 M in THF) over 1 hour. The reaction was allowed to warm to room temperature and a white precipitate gradually appeared. After stirred for 40 h under argon, the precipitate was collected by filtration to give **10** as colorless crystal (2.63 g, 68%). The residue solution was evaporated, and dissolved in $CHCl_3$ and methanol. To this solution was added hexane to give white precipitate. This precipitate was collected, and washed with acetone to give **10** (total yield 82%). m.p. 195-199 °C. ^{1}H NMR (500 MHz, $CDCl_3$, 25 °C): δ = 8.68 (s, 4H), 8.56 (s, 4H), 8.07 (s, 4H), 7.87 (s, 4H) , 5.29 (s, 8H). ^{13}C NMR (125 MHz, $CDCl_3$:CD_3OD = 10:1, 25 °C): δ = 165.6 (*C*q), 151.4 (*C*H), 148.0 (*C*H), 139.7 (*C*H), 134.6 (*C*q), 132.9 (*C*q), 130.4 (*C*H), 121.4 (*C*q), 65.1 (CH_2). IR (KBr): 3070, 3053, 1736, 1719, 1256, 1137, 1101 cm^{-1}. elemental analysis: calcd for **10**. $C_{34}H_{22}Br_4N_4O_8$ (%): C, 43.71.

H, 2.37. N, 6.00. found: C, 43.79. H, 2.50. N, 5.70.

Synthesis of Tetrakis(5,3':5',3"-terpyridin-3-ylmethyl) 1,2,4,5-benzenetetracarboxylate (2)

Under argon, a mixture of **10** (0.40 g, 0.43 mmol), 3-tributylstannyl-5,3'-bipyridine (1.53 g, 3.44 mmol, see ref. [5a] of the text), $Pd(PPh_3)_4$ (0.400 g, 0.034 mmol) in dry toluene (150 mL) was refluxed for 2 d under argon. The mixture was filtered and the residue was purified by column chromatography (aluminium oxide, $CHCl_3$/methanol 40/1) to give **2** as colorless crystal (0.069 g, 13%). m.p. 242-246 °C. ^{1}H NMR (500 MHz, $CDCl_3$:CD_3OD = 10:1, 25 °C): δ = 8.87 (dd, J = 2.4, 0.9 Hz, 4H), 8.86 (m, 12H), 8.67 (d, J = 1.8 Hz, 4H), 8.65 (dd, J = 4.8, 1.5 Hz, 4H), 8.20 (m, 4H), 8.19 (s, 2H), 8.09 (t, J = 2.0 Hz, 4H), 8.05 (dt, J = 8.5, 2.0 Hz, 4H), 7.52 (dd, J = 8.5, 4.8 Hz, 4H), 5.43 (s, 8H). ^{13}C NMR (125 MHz, $CDCl_3$:CD_3OD = 10:1, 25 °C): δ = 165.0 (*C*q), 148.9 (*C*H), 148.8 (*C*H), 147.6 (*C*H), 147.4 (*C*H), 147.2 (*C*H), 147.0 (*C*H), 135.0 (*C*H), 135.0 (*C*H), 133.9 (*C*q), 133.7 (*C*q), 133.2 (*C*H), 133.0 (*C*q), 132.9 (*C*q), 132.8 (*C*q), 131.1 (*C*q), 129.7 (*C*H), 124.0 (*C*H), 64.9 (CH_2). IR (KBr): 3038, 1730, 1719, 1395, 1244, 1128, 1098, 715 cm^{-1}. HRMS (EI): calcd for $C_{74}H_{51}N_{12}O_8$ [M+H$^+$]: 1235.3953. found: 1235.3938.

Self-assembly and physical data of 5•3

1 (10.2 μmol) and **2** (1.7 μmol) were combined in D_2O (0.8 ml) and stirred for 2 h at 70 °C. To this solution, powder of **5** (1.7 μmol) was added and the mixture was stirred at 70 °C for 3 h to give **5•3** in a quantitative yield. ^{1}H NMR (500 MHz, D_2O, 25 °C, TMS): δ = 10.29 (s, 4H. Py*H*), 9.92 (s, 4H. Py*H*), 9.57 (s, 4H. Py*H*), 9.45 (s, 4H. Py*H*), 9.37 (s, 4H. Py*H*), 9.35 (s, 4H. Py*H*), 9.06 (d, J = 6.0 Hz, 4H. Py*H*), 9.03 (s, 4H. Py*H*), 8.41 (s, 2H. Ar*H*), 8.16 (d, J = 6.0 Hz, 4H. Py*H*), 7.61 (t, J = 6.0 Hz, 4H. Py*H*), 5.91 (d, J = 11.4 Hz, 4H. CH_2), 5.31 (d, J = 11.4 Hz, 4H. CH_2), 4.86 (d, J = 7.4 Hz, 2H. **5**·Ar*H*), 4.83 (d, J = 7.4 Hz, 2H. **5**·Ar*H*), 4.50 (d, J = 7.4 Hz, 2H. **5**·Ar*H*), 4.47 (d, J = 7.4 Hz, 2H. **5**·Ar*H*), 3.01–2.79 (m, 24H. $NH_2CH_2CH_2NH_2$), 1.83 (s, 3H. **5**·CH_3), -0.25 (s, 3H. **5**·CH_3). ^{13}C NMR (125 MHz, D_2O, 25 °C, TMS): δ = 165.8 (*C*O), 153.4 (*C*H), 152.4 (*C*H), 149.5 (*C*H), 149.3 (*C*H), 149.0 (*C*H), 148.7 (*C*H), 138.3 (*C*H), 138.1 (*C*q), 137.0 (*C*H), 135.2 (*C*q), 135.1 (*C*q), 134.2 (*C*q), 133.8 (*C*q), 133.6 (*C*q), 133.5 (*C*q), 133.0 (*C*H), 132.0 (*C*q), 131.4 (*C*q), 131.3 (*C*q), 130.3 (*C*H), 128.8 (**5**·*C*H), 127.5 (*C*H), 126.6 (**5**·*C*H), 123.6 (**5**·*C*H), 122.7 (**5**·*C*H), 64.2 (CH_2), 47.3 (CH_2), 47.1 (CH_2), 47.0 (CH_2), 20.2 (**5**·CH_3), 18.0 (**5**·CH_3). CSI-MS of **3** *m/z*: 931.0 $[M-(NO_3)_3]^{3+}$, 682.2 $[M-(NO_3)_4]^{4+}$ (CSI-MS was measured for accommodating naphthalene as a guest.).

Physical data of 6•3

^{1}H NMR (500 MHz, D_2O, 25 °C, TMS): δ = 10.16 (s, 4H. Py*H*), 9.80 (s, 4H. Py*H*), 9.63 (s, 4H. Py*H*), 9.47 (s, 4H. Py*H*), 9.40 (s, 4H. Py*H*), 9.27 (s, 4H. Py*H*), 9.03 (d, J = 5.1 Hz, 4H. Py*H*), 8.90 (s, 4H. Py*H*), 8.53 (s, 2H. Ar*H*), 8.18 (br s, 4H. Py*H*), 7.69 (br s, 4H. Py*H*), 5.92 (d, J = 11.4 Hz, 4H. CH_2), 5.30 (d, J = 11.4 Hz, 4H. CH_2), 5.21 (br s, 2H. **6**·Ar*H*), 4.94 (br s, 2H. **6**·Ar*H*), 4.51 (br s, 2H. **6**·Ar*H*), 4.48 (br s, 2H. **6**·Ar*H*), 4.29 (br s, 1H. **6**·Ar*H*), 3.03–2.79 (m, 24H. $NH_2CH_2CH_2NH_2$). ^{13}C NMR (125 MHz, D_2O, 25 °C, TMS): δ = 165.7 (*C*O), 153.5 (*C*H), 153.1 (*C*H), 149.9 (*C*H), 149.3 (*C*H), 149.2 (*C*H), 149.1 (*C*H), 138.4 (*C*H), 137.0 (*C*H), 135.1 (*C*q), 133.8 (*C*q), 133.7 (Cq), 132.8 (*C*H), 131.9 (*C*q), 131.6 (*C*q), 131.1 (*C*q), 130.2 (*C*H), 128.5 (**6**·*C*H), 127.6 (*C*H), 126.4 (**6**·*C*H), 123.6 (**6**·*C*H), 122.8 (**6**·*C*H), 64.3 (*C*H$_2$), 47.3 (*C*H$_2$), 47.1 (*C*H$_2$), 47.0 (*C*H$_2$) (Guest signals were not clearly observed due to low S/N ratio.). CSI-MS of **6•3** *m/z*: 1494.6 $[M–(NO_3)_2]^{2+}$, 975.7 $[M–(NO_3)_3]^{3+}$.

Physical data of 6•4

m.p. 242 °C dec.. ^{1}H NMR (500 MHz, D_2O, 25 °C, TMS): δ = 10.15 (s, 8H. Py*H*), 9.89 (s, 8H. Py*H*), 9.81 (s, 8H. Py*H*), 9.60 (s, 8H. Py*H*), 9.46 (s, 8H. Py*H*), 9.11 (d, J = 5.4 Hz, 8H. Py*H*), 9.06 (s, 8H. Py*H*), 8.68 (s, 8H. Py*H*), 8.33 (d, J = 7.5 Hz, 8H. Py*H*), 8.11 (s, 4H. Py*H*), 7.79 (t, J = 7.5 Hz, 8H. Py*H*), 6.24 (m, 2H. **6**·Ar*H*), 5.90 (d, J = 13.2 Hz, 8H. CH_2), 5.75 (d, J = 13.2 Hz, 8H. CH_2), 5.71 (d, J = 6.3 Hz, 4H. **6**·Ar*H*), 5.40 (m, 4H. **6**·Ar*H*), 4.98 (m, 4H. **6**·Ar*H*), 3.01–2.79 (m, 48H. $NH_2CH_2CH_2NH_2$) (Some guest signals were unclear due to signal overlap.). IR (KBr) 3459, 3212, 3089, 1735, 1352, 1127, 1098, 1059 cm^{-1}. elemental analysis: calcd for **(6)$_2$•4**. $(C_{172}H_{196}N_{72}O_{88}Pd_{12})\cdot(C_{13}H_9NaO_2)_2\cdot 45H_2O$ (%): C, 32.99. H, 4.25. N, 13.99. found: C, 32.65. H, 3.91. N, 14.37.

Crystal data of (6)$_2$•4

(6)$_2$•4 ($C_{202}H_{218}N_{72}O_{119}Pd_{14}$, Mw = 7048.08): crystal dimensions 0.40 x 0.20 x 0.20 mm^3, triclinic, $P\bar{1}$, a = 16.494(4), b = 16.610(4), c = 31.977(8) Å, α = 78.438(5), β = 86.281(5), γ = 70.333(4)°, V = 8082(3) Å^3, Z = 1, ρ_{calcd} = 1.438 mg m^{-3}, F(000) = 3482, radiation, λ(Mo$_{K\alpha}$) = 0.71073 Å, T = 113(2) K, reflections collected/unique 51758/35688 (R_{int} = 0.0585). The structure was solved by direct methods (SHELXL-97) and refined by full-matrix least-squares methods on F^2 with 1658 parameters. R_1 = 0.1255 ($I > 2\sigma(I)$), wR_2 = 0.3444, GOF = 1.149, max/min. residual density 3.141/-3.798 e Å^{-3}. Several water, nitrate molecules, and ethylene diamine ligands are disordered. Guest molecules sit on two positions (1:1 ratio) in the cavity of a host molecule. The thermal temperature factors of some disordered groups were constrained. The bond lengths of severely disordered molecules were chemically restrained.

Crystallographic data (excluding structure factors) for the structure reported in this paper were deposited with the Cambridge Crystallographic Data Centre as supplementary publication no. CCDC-204999.

8.5 References

1 For reviews: (a) I. Huc, J.-M. Lehn, *Proc. Natl. Acad. Sci. USA* **1997**, *94*, 2106–2110. (b) J.-M. Lehn, *Chem. Eur. J.* **1999**, *5*, 2455–2463. (c) G. R. L. Cousins, S.-A. Poulsen, J. K. M. Sanders, *Curr. Opin. Chem. Biol.* **2000**, *4*, 270–279. (d) S. J. Rowan, S. J. Cantrill, G. R. L. Cousins, J. K. M. Sanders, J. F. Stoddart, *Angew. Chem.* **2002**, *114*, 938–993. *Angew. Chem. Int. Ed.* **2002**, *41*, 898–952.

2 (a) M. Fujita, S. Nagao, K. Ogura, *J. Am. Chem. Soc.* **1995**, *117*, 1649–1650. (b) B. Hasenknopf, J.-M. Lehn, N. Boumediene, A. Dupont-Gervais, A. V. Dorsselaer, B. Kneisel, D. Fenske, *J. Am. Chem. Soc.* **1997**, *119*, 10956–10962. (c) B. Klekota, M. H. Hammond, B. L. Miller, *Tetrahedron Lett.* **1997**, *38*, 8639–8642. (d) M. Scherer, D. L. Caulder, D. W. Johnson, K. N. Raymond, *Angew. Chem.* **1999**, *111*, 1690–1694. *Angew. Chem. Int. Ed.* **1999**, *38*, 1588–1592. (e) M. Albrecht, O. Blau, R. Fröhlich, *Chem. Eur. J.* **1999**, *5*, 48–56. (f) S. Hiraoka, M. Fujita, *J. Am. Chem. Soc.* **1999**, *121*, 10239–10240. (g) Y. Kubota, S. Sakamoto, K. Yamaguchi, M. Fujita, *Proc. Natl. Acad. Sci. USA* **2002**, *99*, 4854–4856. (h) S. Otto, R. L. E. Furlan, J. K. M. Sanders, *Science* **2002**, *297*, 590–593.

3 (a) G. W. Orr, L. J. Barbour, J. L. Atwood, *Science* **1999**, *285*, 1049–1052. (b) M. Ziegler, J. J. Miranda, U. N. Andersen, D. W. Johnson, J. A. Leary, K. N. Raymond, *Angew. Chem.* **2001**, *113*, 755–758. *Angew. Chem. Int. Ed.* **2001**, *40*, 733–736. (c) S. Hiraoka, T. Yi, M. Shiro, M. Shionoya, *J. Am. Chem. Soc.* **2002**, *124*, 14510–14511. (d) C.-Y. Su, Y.-P. Cai, C.-L. Chen, F. Lissner, B.-S. Kang, W. Kaim, *Angew. Chem.* **2002**, *114*, 3519–3523. *Angew. Chem. Int. Ed.* **2002**, *41*, 3371–3375.

4 Ligand **2** was synthesized as follows. The Mitsunobu esterification of tetracarboxylic acid **8** with alcohol **9** gave tetrabromide precursor **10** (82%), which subsequently treated with stannylbipyridine under the Stille coupling conditions [$Pd(PPh_3)_4$ (10 mol%), toluene, reflux] to give **2** in 13% yield.

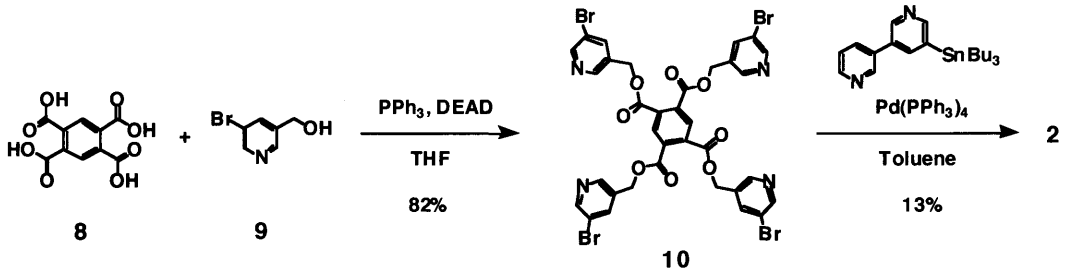

5 (a) M. Aoyagi, K. Biradha, M. Fujita, *J. Am. Chem. Soc.* **1999**, *121*, 7457–7458. (b) M. Aoyagi, S. Tashiro, M. Tominaga, K. Biradha, M. Fujita, *Chem. Commun.* **2002**, 2036–2037. (c) M. Tominaga, S. Tashiro, M. Aoyagi, M. Fujita, *Chem. Commun.* **2002**, 2038–2039.

6 (a) I. Tabushi, K. Shimokawa, N. Shimizu, H. Shirakata, K. Fujita, *J. Am. Chem. Soc.* **1976**, *98*, 7855–7856. (b) S. Zhao, J. H. T. Luong, *J. Chem. Soc., Chem. Commun.* **1995**, 663–664. (c) D. Whang, J. Heo, J. H. Park, K. Kim, *Angew. Chem.* **1998**, *110*, 83–85. *Angew. Chem. Int. Ed.* **1998**, *37*, 78–80. (d) T. Heinz, D. M. Rudkevich, J. Rebek, Jr., *Nature* **1998**, *394*, 764–766. (e) S. Saito, C. Nuckolls, J. Rebek, Jr., *J. Am. Chem. Soc.* **2000**, *122*, 9628–9630.

7 (a) S. Sakamoto, M. Fujita, K. Kim, K. Yamaguchi, *Tetrahedron* **2000**, *56*, 955–964. (b) Y. Yamanoi, Y. Sakamoto, T. Kusukawa, M. Fujita, S. Sakamoto, K. Yamaguchi, *J. Am. Chem. Soc.* **2001**, *123*, 980–981.

8 CSI-MS was measured for complex **3** accommodating biphenylcarboxylate or naphthalene as a guest. A series of $[M\text{-}(NO_3)_n]^{n+}$ peaks were observed.

9 At 80 °C, broad methyl signals were observed indicating that coalesce temperature is nearing.

10 T. Kauffmann, H. Fischer, *Chem. Ber.* **1973**, *106*, 220.

Conclusion

I demonstrated the peptide recognition by using the self-assembled coordination cages. ***In chapter 1***, I advocated that the self-assembled cages are ideal peptide receptors for the sequence-selective recognition and the control of peptide secondary structures via recognition. Because, the cages possess large, hydrophobic cavities enough to fully accommodate oligopeptides in water. Indeed, the coordination cages exhibited the sequence-selective recognition of a tripeptide as ***in chapter 2***. The cages fully accommodate a tripeptide, such as Trp-Trp-Ala in a highly selective fashion in water. Multiple interaction, such as CH-π and π-π interactions between cages and peptides was important for this selectivity. ***In chapter 3***, porphyrin cage showed very strong affinity with a tripeptide, Tyr-Tyr-Ala even in water. The association constants were comparable with those of biological recognition system such as antibody-antigen. ***In chapter 4***, I demonstrated that α-helical conformation of a 9-residue peptide was stabilized by encapsulation within bowl-shaped cavity. This peptide was bound in the cavity through hydrophobic binding in water. The full encapsulation of the 9-residue peptide within the dimeric capsule of bowl-shaped cavity was described ***in chapter 5***. In this case, the peptide also folded into α-helical conformation in the capsule. ***In chapter 6***, the stabilization of a minimal helix, namely a β-turn structure in water was described. A tripeptide Ala-Ala-Ala was fully accommodated within the cavity of porphyrin cage and folded into β-turn structure. ***In chapter 7 and 8***, I demonstrated the design of dynamic peptide receptors by using the self-assembled system via coordination.

From those results of peptide recognition in this thesis, I consider that the self-assembled cages are one of the ideal peptide receptors, which can comparable with biological recognition systems. Finally, I expect that the these self-assembled cages will regulate various vital functions, such as protein-protein interaction, through selective and strong recognition of peptide sequence on the protein surfaces.

List of Publications

"Peptide Recognition: Encapsulation and α-Helical Folding of a Nine-Residue Peptide within a Hydrophobic Dimeric Capsule of a Bowl-Shaped Host" (Chapter 5)
S. Tashiro, M. Tominaga, Y. Yamaguchi, K. Kato, M. Fujita, *Chem. Euro. J.*, **2006**, *in press*

"Folding a de novo Designed Peptide into α-Helix through Hydrophobic Binding by a Bowl-Shaped Host" (Chapter 4)
S. Tashiro, M. Tominaga, Y. Yamaguchi, K. Kato, M. Fujita, *Angew. Chem. Int. Ed.*, **2006**, *45*, 241

"Sequence-Selective Recognition of Peptides within the Single Binding Pocket of a Self-Assembled Coordination Cage" (Chapter 2)
S. Tashiro, M. Tominaga, M. Kawano, B. Therrien, T. Ozeki, M. Fujita, *J. Am. Chem. Soc.*, **2005**, *127*, 4546

"Pd(II)-Directed Dynamic Assembly of a Dodecapyridine Ligand into End-Capped and Open Tubes: The Importance of Kinetic Control in Self-Assembly" (Chapter 8)
S. Tashiro, M. Tominaga, T. Kusukawa, M. Kawano, S. Sakamoto, K. Yamaguchi, M. Fujita, *Angew. Chem. Int. Ed.*, **2003**, *42*, 3267

"Spectroscopic and Crystallographic Studies on the Stability of Self-assembled Coordination Nanotubes"
M. Aoyagi, **S. Tashiro**, M. Tominaga, B. Kumar, M. Fujita, *Chem. Commun.*, **2002**, 2036

"Dynamic Aspects in Host-Guest Complexation by Coordination Nanotubes" (Chapter 7)
M. Tominaga, **S. Tashiro**, M. Aoyagi, M. Fujita, *Chem. Commun.*, **2002**, 2038

General Experimental Section

Materials

Organic solvents and reagents were purchased from TCI Co., Ltd., WAKO Pure Chemical Industries Ltd., and Aldrich chemical., Ltd. Deuterated solvents were acquired from Cambridge Isotope Laboratories, Inc. Fmoc amino acids and some reagents for the peptide synthesis were purchased from Watanabe chemical industries Ltd.

Peptide synthesis

Peptides were synthesized by an automated peptide synthesizer (ABI 433A, Applied Biosystems) using the standard Fmoc-based FastMoc coupling chemistry (0.1 mmol scale). Peptides were cleaved from the resin with TFA (10 mL) containing 5% (v/v) water and 5% (v/v) 1,2-ethanedithiol as a scavenger at room temperature for 3 h. Free peptides were washed from the resin subsequently with TFA (3 mL) and dichloromethane (5 mL). After evaporation, a large amount of Et_2O was added to the residue and the precipitate was collected by filtration. Crude peptides were purified by reversed-phase HPLC on an Inertsil Peptides C18 (GL Sciences Inc.) semi-preparative column (20 mm x 250 mm) using 10 mM ammonium hydrogencarbonate solution with 0.05% TFA (pH 6.0) and acetonitrile gradient, or aqueous 0.1% TFA and acetonitrile gradient. Then white powder of peptides was obtained by lyophilization. Characterization of peptides was carried out by ^{1}H NMR and MALDI-TOF mass (Voyager-DE STR, Applied Biosystems).

UV titration

A peptide was dissolved in water under sonication and the solution was filtered by a disk-filter to remove trace amount of insoluble impurities. The concentration of peptide was determined by the absorption of Trp or Tyr residues.[1] A 3.0 mL of peptide solution was placed in a 1 cm quartz cell. The concentrated aqueous solution of self-assembled host was added in portions via microsyringe to the cell. Absorption spectra were recorded on a SHIMADZU UV-3150 spectrometer. All titrations were carried out at room temperature under appropriate buffers. The association constant was calculated by a nonlinear curve-fitting procedure.[2]

Job's plot

Equimolar solutions of host and peptide were mixed in various ratios. Absorption spectra

were measured and charge-transfer band at 430 nm or 480 nm were analyzed by the Job's method.[2,3]

NMR spectroscopy

NMR spectra were recorded on Bruker Avance 600 spectrometer or Bruker DRX 500 spectrometer. TOCSY and NOESY were measured in phase-sensitive mode. Mixing time of TOCSY was 80 ms and NOESY was 250 ms or 300 ms. For water signal suppression, a WATERGATE solvent suppression scheme was applied to most NMR experiments.[4] DOSY spectra were recorded on a Bruker DRX 500 spectrometer at 300 K with a z axis gradient amplifier. All spectra were processed using XWINNMR (Bruker).

Structural calculation by CNS

Conformation of bound peptides were calculated with the program CNS 1.1.[5] Distance restraints were estimated from the cross-peak intensities in NOESY. Pseudo-atom corrections were used for methyl and methylene protons, according to the protocol of CNS. Backbone dihedral angle restraints were inferred from $^3J_{NHC\alpha}$ coupling constants. For $^3J_{NHC\alpha} < 6$ Hz, ϕ was restrained to $-65 \pm 25°$. No restraints were included for residues with $6 < \phi < 8.5$ Hz because of the problem of multiple solutions to Karplus equation over this range. Structures were displayed using MacroModel (Schrödinger, Inc.). Analysis of RMSD to mean coordinates was performed with the program MOLMOL.[6]

NMR competition experiment for the estimation of binding constants

In NMR competition experiment, if binding constant between guest1 and host is known, binding constant between guest2 and host can be estimated by this equation,

$$K_{a2} = \frac{(1 - x)([guest_1]_0 - x)}{x\{[guest_2]_0 - (1 - x)\}} K_{a1}$$

where K_{a1} or K_{a2} are binding constant between host and guest1 or guest2 respectively, $[guest_1]_0$ or $[guest_2]_0$ are initial concentration of guest1 or guest2 respectively, and x is concentration of [host•guest1]. The x can be calculated by integration ratio of host•guest1 and host•guest2 in ^{1}H NMR, when these host-guest equilibriums are slow enough in NMR time scale. It is also necessary that concentration of free host species is almost zero for the estimation of x by integration ratio.

References

1 J. F. Brandts, L. J. Kaplan, *Biochemistry*, **1973**, *12*, 2011.

2 K. A. Connors, *Binding Constants–The Measurement of Molecular Complex Stability*, Wiley, New York, **1987**.

3 P. Job, *Compt. Rend.* **1925**, *180*, 928.

4 M. Piotto, V. Saudek, V. Sklenar, *J. Biomol. NMR* **1992**, *2*, 661.

5 A. T. Brünger, *et al.*, *Acta. Cryst.*, **1998**, *D54*, 905.

6 R. Koradi, M. Billeter, K. Wüthrich, *J. Mol. Graph.*, **1996**, *14*, 51.

Acknowledgments

The author is sincerely grateful to his supervisor, Professor Makoto Fujita, for six years. He sincerely thanks for his a lot of fruitful advices and encouragements.

He deeply thanks to Dr. Masahide Tominaga for continuous encouragements and his leading. He also thanks to Assoc. Prof. Masaki Kawano for X-ray studies and various helps. He thanks to Dr. Michito Yoshizawa for various discussions and encouragements. He also thanks to Assoc. Prof. Takahiro Kusukawa for several NMR and X-ray measurements and various discussions. He thanks to Dr. Akiko Hori and Assoc. Prof. Takashi Okano for their encouragements.

He gratefully thanks to Professor Mitsuhiko Shionoya for various encouragements and supports.

He deeply thanks to his co-worker Mr. Masahide Kobayashi for a lot of help. Especially, studies about porphyrin cage in this thesis were carried out by him. His acknowledgments are also due to his co-workers Mr. Keigo Inaba for peptide studies, and Mr. Takumi Yamaguchi for studies about tubular complex. He also thanks to Dr. Kanji Takaoka for his encouragements and pleasurable three years as same PhD students.

He thanks to Prof. Kentaro Yamaguchi and Dr. Shigeru Sakamoto for CSI-MS studies. He also thanks to Assoc. Prof. Tomoji Ozeki and Dr. Bruno Therrien for X-ray measurement and analysis. His acknowledgments are also due to Prof. Koichi Kato and Dr. Yoshiki Yamaguchi for NMR measurements and fruitful advices.

He thanks to all the members of Fujita laboratory at Nagoya University and the University of Tokyo. He also thanks to JSPS.

Finally, he thanks to his parents for everything.